Alma Mater Studiorum – Università di Bologna

Dipartimento di Medicina Specialistica, Diagnostica e Sperimentale

Dottorato di Ricerca in Oncologia, Ematologia e Patologia

Coordinatore Prof. Pier-Luigi Lollini

XXXI Ciclo

Scientifico Disciplinare: MED/15

Settore Concorsuale:06/D3

Exploiting genomic instability in Acute Myeloid Leukemia: when *TP53* fails.

Presentata da: **Maria Chiara Fontana**

Coordinatore Prof. Pier-Luigi Lollini

Supervisore: Dott.ssa Simona Soverini

Co-supervisore: Prof. Giovanni Martinelli

Esame finale anno 2019

SUMMARY

ABSTRACT

Acute myeloid leukemia (AML) is a myeloid neoplasm with a heterogenic genomic background and a poor prognosis. Understanding which genomic abnormalities and biomarkers are responsible for poor prognosis in AML is still a need. The main aims of this thesis are to deepen the pathogenic mechanism of genomic instability (1) and drug-resistance (2) p53-related, in order to identify new targets and biomarker of response through genomic and in vitro approaches.

(1) A peculiar mechanism of genomic instability is chromothripsis, a one-step genome-shattering catastrophe resulting from disruption of one or few chromosomes in multiple fragments and consequent random rejoining and repair. The main purpose of this study was to define the incidence of chromothripsis in 395 newly-diagnosed adult AML patients from three Institutions, its impact on survival and its genomic background using SNP 6.0 or Cytoscan HD Array (Affymetrix®). Chromothripsis was detected with a custom algorithm in 26/395 patients. Patients harboring chromothripsis had higher age (p = .002), ELN2107 high risk (HR), lower white blood cell (WBC) count, *TP53* loss and/or mutations while *FLT3* and *NPM1* mutations were mutually exclusive with chromothripsis. Patients with chromothripsis showed a worse overall-survival (OS) even compared with HR patients, moreover chromothripsis significantly defined prognosis in a COX-HR optimal regression model. In comparison to chromothripsis-negative patients, chromothripsis-positive patients presented the hallmarks of chromosome instability [i.e. *TP53* alteration, 5q deletion, a higher mean of copy number alteration (CNA), complex karyotype, alterations in DNA repair and cell cycle]. CBA and FISH showed that chromothripsis was associated with marker, derivative and ring chromosomes.

(2) *PPM1D* is a promising oncogene coding for "Wild type p53-Inducible Phosphatase 1" (WIP1) which negatively regulates p53 and several proteins involved in the DNA damage response (DDR). It has been proposed to be a primary homeostatic regulator of the DDR pathway by facilitating the return to steady state after DNA damage. A recent study[1] has demonstrated that *PPM1D* inhibition with GSK2830371 reverses chemotherapy resistance to cytarabine and selectively targets *PPM1D*-mutant AML cells in vitro and in vivo. The aim of this work is to investigate whether the inhibition of WIP1 by GSK2830371 could increase the sensitivity to MDM2 inhibitors (e.g. Nutlin-3a) in order to obtain a novel therapeutic strategy for AML patients restoring p53 activity. Our study showed that in vitro pharmacological inhibition of WIP1 by GSK2830371 potentiates the sensitivity to Nutlin-3a, a MDM2 inhibitor, in AML cells by stabilizing the activity of p53 by activating apoptosis and other p53-downstream genes and pathways, as confirmed by gene expression profile (GEP) and western blot (WB) analyses of treated AML cells.

INTRODUCTION

1. Acute myeloid leukemia

AML is a neoplastic disease characterized by a defective regulation of the differentiation and self-renewing properties of hematopoietic stem cells located in bone marrow (BM), resulting in an uncontrolled expansion in BM, peripheral blood (PB) and other tissues, of the myeloid precursors cells with an abnormal differentiation capacity and a powerful proliferation [2].

AML is the most common type of acute leukemia in adults, accounting for 80% of all cases of leukemia. The median age at diagnosis is approximately 65 years, but the incidence increases with age: over 65 years the 5-year survival is less than 30%. [3] A further increase is expected from the rising incidence of therapy-related myeloid neoplasms (i.e. myelodysplastic syndromes or AML occurring in cancer survivors after successful treatment of a primary tumor).

In majority of cases AML is a *de novo* disease without a clear etiology. However, several agents, able to induce a DNA damage, have been associated with leukemia pathogenesis: physical agents (radiations), life style, chemical agents, drugs and viruses. Moreover, in rare cases, AML in adults is associated with familial genetic abnormalities (e.g., trisomy 21; Fanconi Anaemia; Bloom's syndrome; familial mutations of *CEBPA*, *DDX41*, *RUNX1*).

Different studies on AML pathogenesis allowed to develop a "two-hit model" of leukemogenesis.[3]

This model includes class I mutations that activate signal transduction pathways and confer a proliferation advantage on hematopoietic cells, and class II mutations that affect transcription factors and primarily serve to impair hematopoietic differentiation and cell apoptosis.[4,5]

The diagnosis of AML requires a BM infiltration of at least 20 percent of the total cells of the BM aspirate (from a 500-cell differential count). Exceptions to this include leukemias with certain genetic abnormalities, such as those with t(8;21), inv(16), or t(15;17), and myeloid sarcoma, which are considered diagnostic of AML without regard to the blast count. Then, leukemic cells must be of myeloid origin as demonstrated by either the presence of Auer rods, cytochemical positivity for myeloperoxidase, or presence of sufficient myeloid/monocytic markers recognized by immunophenotyping.[6,7]

1.2 WHO classification of AML

AML is classified by the World Health Organization system, which is based upon a combination of morphological, immunophenotypical, genetic, and clinical features. The French-American-British

(FAB) classification divides AML into eight subtypes, based on cell morphology defined by cytologic and cytochemical analyses in Table i1. [7]

Table i1. AML FAB classification

FAB	Definition	Cytogenetics
M0	AML, minimally differentiated	
M1	AML, without maturation	
M2	AML, with granulocytic maturation	t(8;21)(q22;q22)t(6;9)
M3	Acute Promyelocitic Leukemia (APL)	t(15;17)
M4	Acute myelomonocitic leukemia	inv(16)(p13q22),del(16q)
M4eos	Myelomonocitic with BM eosinophilia	inv(16),t(16;16)
M5	Acute monoblastic leukemia (M5a) or monocitic leukemia (M5b)	del(11q),t(9;11),t(11;19)
M6	Acute erythroleukemia (M6a) or rare erythroid leukemia (M6b)	
M7	Acute megakaryoblatic leukemia	t(1;22)

The classification tries to identify different biologic entities in the hopes that future work will describe molecular pathways that could be targets of new therapies. In 2016, the World Health Organization (WHO) provided an updated classification system incorporating morphology, cytogenetics, molecular genetics and immunological markers. [7]

1. AML with recurrent genetic abnormalities
2. AML with myelodysplasia-related features
3. Therapy-related AML and MDS
4. AML, not otherwise specified
5. Myeloid sarcoma
6. Myeloid proliferations related to Down syndrome[8,9]

AML with recurrent genetic abnormalities, e.g. – The molecular pathogenesis of AML with inv(3)(q21.3q26.2)or t(3;3)(q21.3;q26.2) was revisited showing that repositioning of a *GATA2* enhancer element leads to overexpression of the *MECOM* (EVI1) gene and to haploinsufficiency of *GATA2*. A new provisional entity "AML with BCR-ABL1" was introduced, while AML with mutated *NPM1* and AML with biallelic mutations of CEBPA have officially become full entities. Finally, a new provisional entity "AML with mutated *RUNX1*" was added and it has been associated with poor outcome. [7–9]

AML with myelodysplasia-related features - Presence of dysplasia of multiple myeloid lineage, pre-existing myeloid disorder, and/or myelodysplasia-related cytogenetic alterations represent diagnostic criteria for this disease category. Particularly, those cytogenetic changes are: complex karyotype (defined as 3 or more chromosomal abnormalities in the absence of one of the WHO-designated recurring translocations or inversions, as: t(8;21), inv(16) or t(16;16), t(9;11), t(v;11)(v;q23.3), t(6;9), inv(3) or t(3;3); AML with BCR- ABL1); unbalanced abnormalities, as: -7 or del(7q); -5 or del(5q); i(17q) or t(17p); -13 or del(13q); del(11q); del(12p) or t(12p); idic(X)(q13); balanced abnormalities: t(11;16)(q23.3;p13.3); t(3;21)(q26.2;q22.1); t(1;3)(p36.3;q21.2); t(2;11)(p21;q23.3); t(5;12)(q32;p13.2); t(5;7)(q32;q11.2); t(5;17)(q32;p13.2); t(5;10)(q32;q21.2); t(3;5) (q25.3;q35.1). [7–9]

Therapy-related AML and MDS - Therapy-related myeloid neoplasms (t-MNs) are defined as myeloid neoplasms appearing after cytotoxic therapy, that may be further subdivided in therapy-related MDS and AML (t-MDS or t-AML), usually associated with recurrent cytogenetic abnormalities.[9]

AML, not otherwise specified - The original subgroup acute erythroid leukemia, erythroid/myeloid type was removed and even if French-American-British (FAB) sub-classification does not seem to provide prognostic information for "AML, NOS" cases if data on *NPM1* and *CEBPA* mutations can be achieved, the 2016 revision agreed to maintain the AML, NOS subcategories as a distinct subgroup [7–9].

Finally, the recent WHO classification introduces a new category of AML: **Myeloid neoplasms with germline predisposition**. Several studies, in fact, showed that in some cases of myeloid neoplasms, including myelodysplastic syndrome (MDS) and AML, inherited or de novo mutations can be found in germ line cells. [7,9]

1.3 Prognosis and Risk stratification

Many factors contribute to the prognosis of AML: pre-treatment factors, which in turns could be patient- or disease-related, treatment-related factors and post-treatment factors, such as MRD[7].

Based on conclusions of different studies[10–12], genomic lesions are responsible of about two-thirds of explained variation, with the other third depending by demographic, clinical, and treatment variables. Although clinical factors have to be considered, genomic alterations constitute the most important prognostic factor for CR and OS in AML. Thus, in 2017 an international expert panel decided to produce an AML risk-stratification scheme based on genetic, in order to guide the clinical practice and the management of patients. The European Leukemia Net (ELN) system distinguishes 3 different

groups: favorable risk, intermediate risk and adverse risk (**Figure i1**). [8]

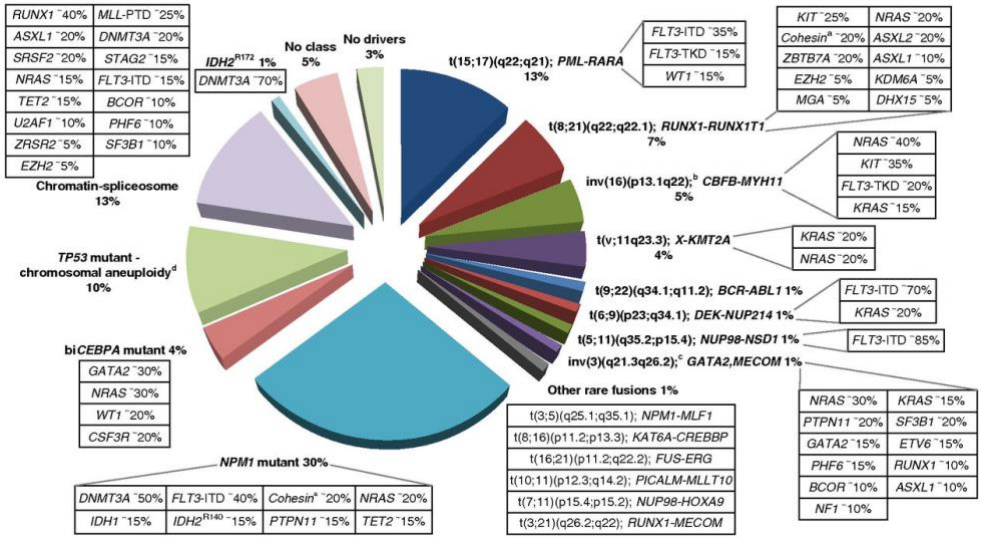

Figure i1. Molecular classes of AML according to 2017 ELN recommendations [7]. For each molecular subgroup, the frequency across AML, and co-occurring mutations with their relative frequency are shown in the boxes.

However, the deep molecular characterization of Papaemmanuil study [10] considering 1540 patient with AML revealed that the prognostic consequence of driver mutations is strongly dependent by the genomic context in which they occur. For instance, the presence of concurrent mutations in patients with *NPM1* or *CEBPA* biallelic mutations, could modify the prognosis. Particularly, the presence of the combined genotype including *NPM1*, *DNMT3A*, and *FLT3*^{ITD} had a deleterious effect on prognosis, while the absence of mutations in at least one of these genes had a less impact. In contrast, the *NPM1–DNMT3A–NRAS*$^{G12/13}$ genotype showed a benign prognosis in this cohort[10]. Apparently, the clinical effect of *CEBPA* or *NPM1* mutations is not modified by the presence of coincidental chromosomal alterations[13]. In general, it is possible to affirm that most recent studies suggest that patients with *NPM1* mutation and *FLT3-ITD* with a low (<0.5) allelic ratio have a similar (favourable) outcome as patients with a *NPM1* mutation but no *FLT3-ITD*, and both groups are now considered favorable[7,14–17]. Considering core-binding factor (CBF) AML, in particular AML with t(8;21), it has been demonstrated that the presence of *KIT* mutations, especially if higher mutant *KIT* levels are present, appears to be associated with poorer prognosis[18–22]. Nevertheless, presence of a *KIT* mutation should not assign a patient to a different genetic risk category.

RUNX1 mutations, for example identify patients with unfavourable prognosis[10,12,23,24]. *ASXL1* mutations increase with age and are associated with inferior survival, too[10,11,25–27]. *TP53* mutations are often associated with complex karyotype (three or more unrelated chromosome abnormalities, in the absence of one of the WHO-designated recurring translocations or inversions), monosomal karyotype (one single monosomy, excluding loss of X or Y, in association with at least one additional monosomy or structural chromosome abnormality, excluding core-binding factor AML)[28–32] and specific chromosomal aneuploidies (eg, -5/5q-, -7/7q-), and prefigure a very poor outcome[10,33,34]. *TP53* mutation and complex karyotype provide independent prognostic information, with the combination of both having the worst outcome[10].

Concerning genes as *DNMT3A, IDH1*, *IDH2*, or genes in the chromatin/spliceosome group[10] other than *ASXL1* and *RUNX1*, the panel of expert did not identified enough strong evidence to assign them to an ELN prognostic group.[7]

1.4 Genomic background of AML

In the last few years, the development of Next Generation Sequencing (NGS) technologies for high-resolution analysis of cancer genome has dramatically improved our understanding of AML pathogenesis, showing that a number of genetic hits participate to the malignant transformation of hematopoietic stem-progenitor cells. It has been demonstrated that the landscape of somatic alterations is the results of a relative small number of "driver mutations" which typically occur with "passenger mutations", thus contributing to the mutational spectrum of genetic variation of leukemic cells.

By analyzing the genome of 200 AML patients, 9 functional categories of significantly mutated genes and their distinct patterns of cooperativity and mutual exclusivity, have been defined (transcription factor gene fusions, *NPM1*, tumor suppressor genes, two groups of epigenetic modifier genes, signaling genes, myeloid transcription factor genes, cohesin- complex genes and spliceosome-complex genes; **Figure i2**) [35,36]. However, two additional groups were either without a molecular driver (4%) or with a driver not falling into a class defining-lesion (11%, **Figure i3**) [10].

An average of 5 recurrently mutated genes and 1.5 gene-fusion event per case were identified. Most patients were characterized by clonal heterogeneity at the time of diagnosis, with the presence of both a founding clone and at least one sub-clone.

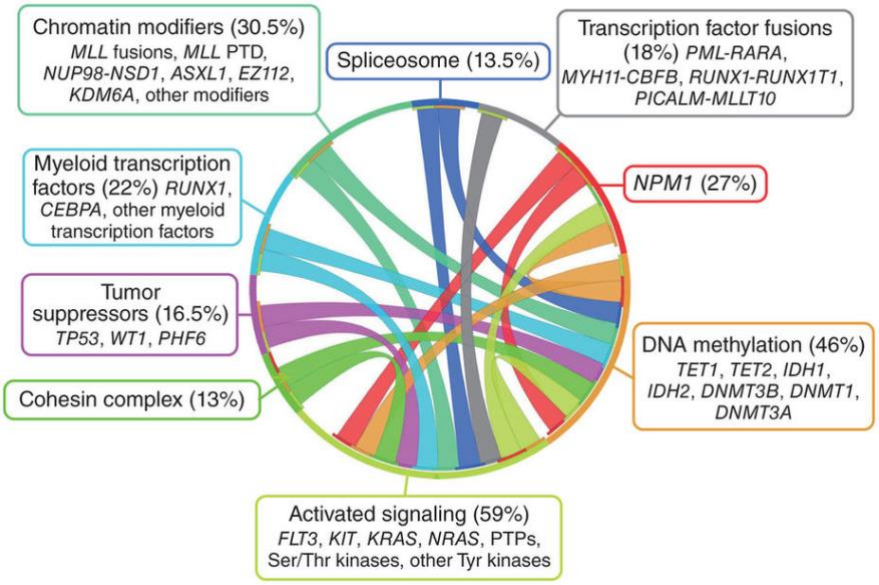

Figure i2. CIRCOS plot showing the 9 functional categories and their pattern of co-occurrence and mutual exclusivity in AML. Ribbons connecting different categories reflect the co-occurency of alterations in genes involved in that pathways. PTPs, protein tyrosine phosphatases; MLL PTD, MLL partial tandem duplication[36].

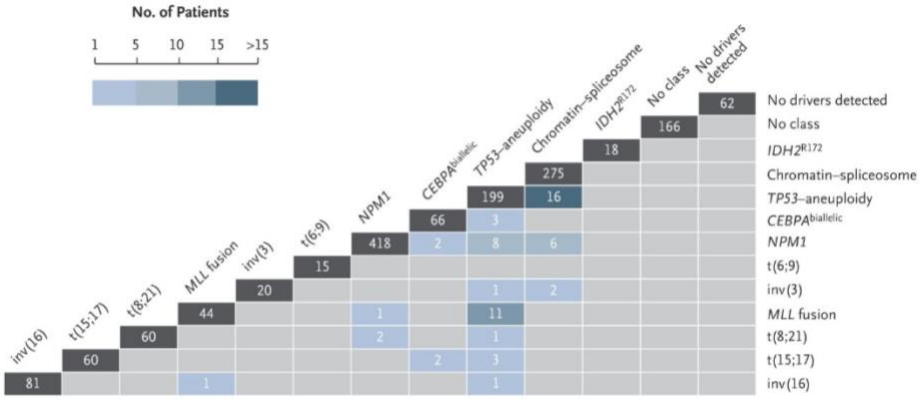

Figure i3. AML molecular subgroups. Patients distribution and intersection across molecular types identified by Papaemmanuil et al [10]. The numbers on the first row of each column represent patients belonging only to the respective class. The numbers along the columns represent patients meeting criteria for more than one subgroup.

Clonal evolution studies on AML demonstrated that genes involved in the epigenetic regulation such as *DNMT3A*, *ASXL1*, *IDH2*, and *TET2* were present in the pre-leukemic clone and persisted during remission, leading to relapse [37]. In addition, two independent studies showed that clonal hematopoiesis occur in healthy individual with somatic mutations involving the same genes

(*DNMT3A, TET2*, and *ASXL1*), increase as people age and were associated with an increased risk of hematologic cancer and in all-cause mortlity[38,39].

Xie M. et al. analyzed the blood-derived sequence data from 2,728 individuals from TCGA and discovered 77 blood-specific mutations in cancer-associated genes, the majority being associated with advanced age. Remarkably, 83% of these mutations were from 19 leukemia and/or lymphoma-associated genes, and nine were recurrently mutated (*DNMT3A, TET2, JAK2, ASXL1, TP53, GNAS,* ***PPM1D***, *BCORL1* and *SF3B1*), possibly representing the earliest stages of clonal expansion in hematopoietic stem cells (**Figure i4**). [40]

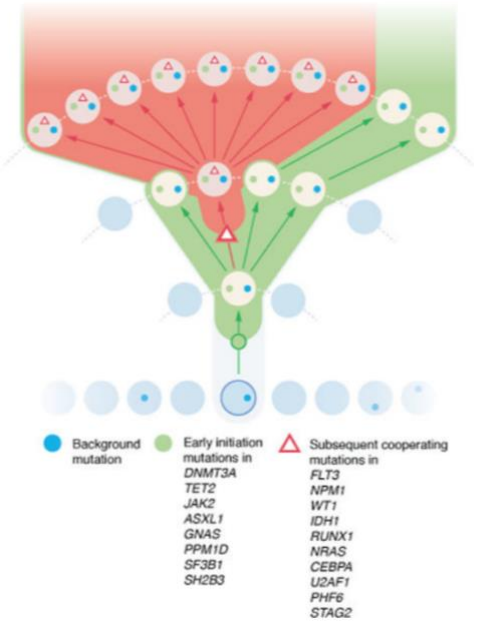

Figure i4. Mutated genes involved in clonal hematopoietic expansion.
The distinct roles of a set of genes including *DNMT3A, ASXL1, TET2, GNAS, JAK2, PPM1D, IDH1, NRAS, NPM1*, and *FLT3* in the initiation of hematopoietic clonal expansion. [40]

Taken together, the deep molecular characterization of AML carried out in the last years helped to re-classify the disease and re-define the diagnosis procedures and the management of patients, as outlined by the 2017 ELN recommendations [7].
Even if the genetic stratification of AML patients has been updated, it still relies on few molecular markers and, most importantly, how this deep molecular characterization of patients may be clinically actionable is still unknown [7].

2. Genomic instability in leukemia

Genomic instability is a common feature of cancer and may result in numerous defects like mitotic replication errors, telomere dysfunction, epigenetic changes or defective DNA repair.

Chromosomal instability is a form of genomic instability, defined by the cell-to-cell variability with regard to chromosomal changes, predisposing to the outgrowth of clones containing "fixed" chromosome aberrations. Chromosome aberrations in myeloid neoplasms include whole-chromosome aberrations like monosomy or trisomy or structural changes like deletions, translocations and inversions. Cytogenetic abnormalities in AML and MDS are associated with distinct clinical and morphological subtypes and often predict disease outcome. Losses of 5q, 7q and 17p are also frequent aberrations of complex karyotypes, which by definition contain three or more clonal aberrations. Chromosomal instability and clonal evolution play an essential role in leukemogenesis by promoting the accumulation of genetic lesions responsible for malignant transformation. [41]

2.1 Chromothripsis and *TP53*

In recent years, the paradigm that genomic abnormalities in cancer cells arise through progressive accumulation of mutational events has been challenged by the discovery of single catastrophic phenomenon called chromothripsis.[42] Chromothripsis involves massive chromosomal rearrangements arising all at once. During chromothripsis, a chromosome or chromosome arm shatters into pieces, followed by incomplete and random repair of the fragments.[42] This can result in a highly rearranged chromosome or chromosomal fragment, whereby certain fragment are lost and/or are incorporated into extrachromosomal double minutes, usually present at high copy numbers. [42] As a result, only two, sometimes three, different copy number states can be detected for each fragment of the chromothriptic chromosome. [42]

Chromothripsis is frequently associate with *TP53* mutations in several cancers [43–51] [52] [53,54,55,56] [57], as well as in germline cases of congenital disorders[58], and complex karyotype and poor overall survival in AML.[59]

As *TP53* is required for the induction of cell cycle arrest, DNA repair and apoptosis following DNA damage, *TP53* inactivation will allow uncontrolled proliferation of cells with DNA damage from chromothripsis. [42] Therefore, a mutation in *TP53* could be predicted to be accompanied by increased incidences of chromothripsis. [42] However, this association is not fully penetrant, in fact chromothriptic rearrangements have been detected in few tumors with wt-*TP53*. [42]

3. *TP53* role in AML

Tumor protein 53 (TP53) is a tumor-suppressor protein encoded by the *TP53* gene located on the short arm of chromosome 17 [60]. In response to multiple cellular stresses, p53 is induced to increase its concentration in nucleus and exert its pro-apoptotic function, incentivizing cell cycle arrest to allow DNA repair and cell death avoiding mitosis of cells with DNA damages [61].

TP53 is mutated in over one-half of human cancers, representing an important mechanism of resistance to DNA-damaging chemotherapeutic agents. [60] The transcription factor encoded by the *TP53* gene is composed of a transcription activation domain, a DNA-binding domain, a proline-rich domain, and a tetramerization domain. [60] Most *TP53* mutations in cancers are located on the DNA-binding domain (exons 5-8). These mutations can either directly disrupt the DNA-binding domain of *TP53* or cause conformational changes of the protein, leading to severely impaired *TP53* function. [60]

In patients with AML, *TP53* mutations are mainly observed in therapy-related AML and/or a complex karyotype (range, 70%-80%), with a frequency from 5% to 10% in patients with de novo AML. [60] In multivariate analyses, the presence of *TP53* mutations without aberrant cytogenetic abnormality predicted for poor OS and inferior response to treatment. [60]
Moreover, 17p loss of heterozygosity, chromosome 17 aberrations, or overexpression of full-length protein isoform also predict an adverse prognosis in patients with AML.[60,62]

At a cytogenetic level, the frequency of complex karyotype is significantly higher in *TP53*-mutated AML patients compared to *TP53*-wild type (wt) patients (81% vs 15%), consistent with previously published reports [34] leading to a phenotype of genomic instability, ineffective DNA repair, and impaired apoptosis. In fact, these patients exhibit lower response rates to intensive chemotherapy and shorter CR durations, translating into inferior survival in both younger and older patients. [60]

Nevertheless, wt p53 dysfunction due to non-mutational p53 abnormalities appears to be rather frequent in various AML entities, bearing a greater impact than is currently appreciated.[63]
Several mechanisms underlying non-mutational wt p53 inactivation, might be of therapeutic relevance. In fact, the adverse cytogenetics and poor outcome, occurring in wt *TP53*-AML with *MDM2/4* or *CRM1* overexpression, suggest that non-mutational wt p53 dysfunction might have significant oncogenic potential.[63] Then, the ARF-MDM2/4-p53 axis is abrogated in most AML cases, undermining wt p53 function due to ARF inactivation and/or *MDM2/4* overexpression (observed in up to 50% AML) ensuing from activated phosphatidylinositol 3-kinase (PI3K)/AKT,

RAS/RAF/MEK/extracellular signal-related kinase (ERK), and NF-kB pathways.[63] NPM1/FLT3-mutated AML is often accompanied by wt p53 dysfunction due to several inactivating processes, in fact *FLT3-ITD* mutations lead to *SIRT1* overexpression, which yields p53 deacetylation, PI3K/AKT pathway activation (promoting MDM2-mediated p53 degradation) predicting poor AML outcome. [63] Then, deregulation of STAT/MAPK pathway leads to Bcl2 accumulation, opposing to p53 activity. [63] Silenced Notch signaling, which is frequently found in AML, is also implicated in wt p53 attenuation. Indeed, Notch agonists were shown to enhance p53 expression along with BCL2 downregulation and growth inhibition of AML cells. [63] Then, some chromosomal translocations, as inv (16)/t(16;16) leads to p53 deacetylation, while deregulations of some miRNA leads to abrogation of p53 function. [63] Finally, truncating mutations of *PPM1D* (WIP1), which normally dephosphorylates p53 at phospho-Ser 15 leads to an overexpression of this protein, turning in a bigger downregulation of p53 function and a chemoresistance phenotype in AML. [1]

For these reasons, a better understanding of the biology of p53 direct or indirect alterations and the mechanism of chemoresistance in AML along with newer approaches to improve the CR rates and prolong survival are critically needed.

4. A novel gene involved in p53 activity regulation with a central role in cell cycle progression and genomic integrity: *PPM1D*

The protein p53 has a critical role in stress response and mediates several anti-proliferative pathways in cells. *PPM1D*, a novel gene originally isolated in a screen for ionizing radiation induced transcripts in Burkitt Lymphoma[64], codes for a Mg^{2+} serine/threonine phosphatase and it is one of the trascriptional target genes of p53. *PPM1D* is also called "Wild Type Induced p53 phosphatase" (WIP1) and its function is increased by ultraviolet (UV), ionizing radiations (IR) and other toxic agents, in a p53 dependent-mechanism[64]. WIP1 protein is involved in DNA damage response and engagement of cell cycle checkpoints, interacting with several substrates in DNA-damage response pathway, as illustrated based on the results from the phosphoproteomic analysis in leukemia cells (Figure i5). [1]

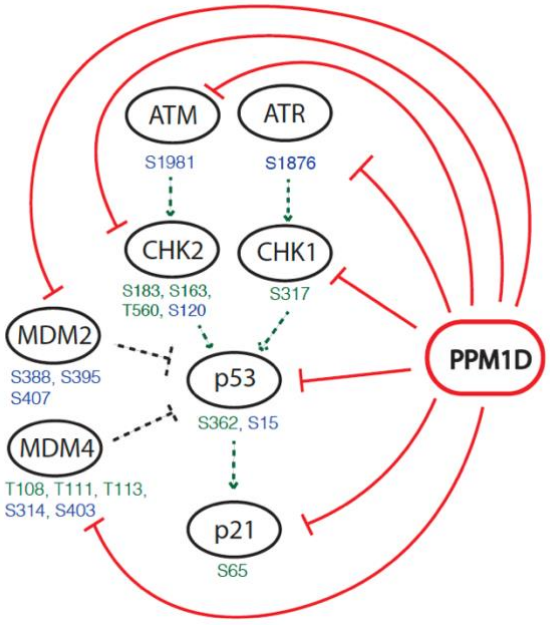

Figure i5. Schema illustrating the components of the DNA-damage response pathway that are targeted by *PPM1D* in leukemia cells. [1]

Different studies demonstrate the capacity of WIP1 to dephosphorylate p53 at Ser 15, the same site where *ATM* and *ATR* explicate their function.[65] Moreover, Chk1 activity is decreased by the dephosphorylation mediated by WIP1, mainly at Ser 345 but in part at Ser 317 too.[65,66] Considering that Chk1 explicate its function by phosphorylating p53, if WIP1 decrease the activity of Chk1, indirectly decrease the activity of p53 too. [65]

The central role of *PPM1D* in cell cycle progression and DNA damage response is not limited to the interaction with p53 and Chk1, even if these are the main pathways, this phosphatase has other targets: historically, the first identified target was p38 MAP kinase, it is usually activated by several genotoxic stress[65], while it is selectively inhibited by *PPM1D*. Furthermore, recent studies have showed the interaction between *PPM1D* and p21, in which WIP1 decrease the activity of p21[67]. Finally, WIP1 has also a role in suppress G2/M checkpoints and in abrogate intra-S-phase checkpoint by interacting directly with specific substrates. [68]

Recent studies showed that WIP1 activity is more growth-promoting than growth-suppressing, appearing to have oncogenic properties in the development of several human cancers. In fact, PPM1D somatic mutations are very frequent in many cancers [69] and in 46% of therapy-related MDS. [70] Truncating mutations in the terminal exon of *PPM1D* have been identified in clonal hematopoiesis and myeloid neoplasms, with a striking enrichment in patients previously exposed to chemotherapy.[39] PPM1D is frequently mutated also in blood of healthy-individuals, in particular in more than 2% of blood of people older than 70 years in association to other mutation related to leukemia found by TCGA (*DNMT3A, TET2, JAK2, ASXL1, TP53, GNAS, PPM1D, BCORL1* and *SF3B1*), this may represent a premalignant initiating event that can cause clonal hematopoietic expansion. [71] [39,40]

Until now, little was known about the role of *PPM1D* in leukemia. A recent study in AML showed that truncating *PPM1D* mutations confer a chemoresistance phenotype, resulting in the selective expansion of *PPM1D*-mutant hematopoietic cells both in vitro and in vivo. [1] CRISPR-Cas9 mutational profiling of *PPM1D* in the presence of chemotherapy selected for the enriched exon 6 mutations identified in patient samples showed that these mutations encode for a truncated protein displaying elevated expression and activity due to loss of a C-terminal degradation domain.
In the presence of chemotherapy, *PPM1D*-mutant cells have an abrogated DDR resulting in altered cell cycle progression, decreased apoptosis, and reduced mitochondrial priming, which could be reversed by a treatment with an allosteric, small molecule inhibitor of *PPM1D* (GSK2830371). In particular, GSK2830371 preferentially kills *PPM1D*-mutant cells, sensitizing cells to chemotherapy reverting the chemoresistance phenotype. [1] Thus, PPM1D's mutations or overexpression, or its activity in general, shed light to its oncogenic properties leading to abnormal proliferation in several cancers, leading to chromosomal instability due to the abrogation of cell cycle checkpoints, and damaged DDR.

5. Therapy of AML

Few innovative therapeutic concepts were effectively translated into the clinical practice and despite some first line therapy success, the prognosis remains poor for a considerable number of cases, which either do not respond to therapy or become incurable when relapsing due to clonal evolution and to the failure of current therapeutic strategies eradicating the leukemia stem cells.

Indeed, chemotherapies have reached their plateau in cure rates and survival in leukemia. Optimal treatment is inpatient-based, highly-toxic and very expensive, involving multiple courses of combination chemotherapy and stem cell transplantation. The aim of the induction therapy is to achieve a CR and it is usually achieved in 60% to 80% of younger adults and in 40% to 60%of older adults (60 years or above)[2,7,72]. The outcome of older patients is even poorer, in particular for those who are considered unfit for intensive chemotherapy. Long-term survival is a dismal 10-20%.

Beside the traditional regimen, new alternative drugs have been evaluated in recent clinical trials giving new perspectives to specific categories of patients. A key problem is how to address the right therapy to any individual patient. Approaches with novel drugs (i.e. hypomethylating agents, monoclonal antibodies, molecular target drugs) are failing in drastically augmenting cure rates and overall survival in general onco-hematological population. The most recent approaches for personalized therapies are aimed at tailoring clinical trials to patients' specific genomic background and response rates are lower than expected.

5.1 Inhibiting MDM2 to restore p53 functionality: WIP1 inhibitor as a new marker for target therapy

Among the categories of novel promising drugs, in particular for relapsed/refractory patients, MDM2 inhibitors represent a promising approach for the treatment of AML.

MDM2 targets p53 for ubiquitination/degradation: higher levels of MDM2 protein expression are consistent with a mechanism of increased malignant potential by decreasing p53 activity[73]. The MDM2 antagonists, called "*nutlins*", act by preventing the link between MDM2 and p53, blocking ubiquination/degradation of p53 and stabilizing the protein to perform its tumor suppressor and transcriptional regulation leading to the activation of apoptotic pathways[74]. Nutlin-3a is the more potent diastereoisomer of racemic MDM2 antagonist Nutlin-3. It was called enantiomer-a since it elutes as the first peak from chiral purification of racemic nutlin-3. Nutlin-3a is a potent inhibitor of MDM2 binding to p53 (with an IC50 of 90 nM) that induces the expression of p53 regulated genes, and shows potent anti-proliferative activity in cells expressing functional p53. Nutlin-3a is 150 times more potent than Nutlin-3b. Cells which have acquired a specific growth advantage thanks to reduced p53

functional activity by amplification or overexpression of MDM2[75] represent a unique paradigm for targeting a co-opted mechanism by oncology therapeutics[76].

Nowadays many clinical trials with MDM2 inhibitors are ongoing or have just been closed with promising results. Idasanutlin (RG7388) is a potent selective MDM2 antagonist showing promising responses in phase I/II studies in relapsed-refractory AML. Currently, the ongoing phase III Roche trial (MIRROS- Hoffman-La Roche) is investigating the superiority of Idasanutlin plus Cytarabine versus Cytarabine plus Placebo (NCT02545283).
Moreover, Idasanutlin is also used in a multi-arm study with Venetoclax (BCL-2 inhibitor) in combination with Cobimetinib (MEK inhibitor), and Venetoclax in combination with Idasanutlin in patients ≥ 60 years with relapsed or refractory AML who are not eligible for cytotoxic therapy (NCT02670044). Due to the preliminary result of these clinical trials, Idasanutlin has been considered a useful drug for patients belonging to the category with a very poor prognosis. However, relapsed/refractory AML are really hard to eradicate, for this reason, Idasanutlin is only one of the option, in fact this drug has good efficacy but the therapy has to be improved.

Another possible target to improve MDM2 inhibition could be represented by the inhibition of *PPM1D*/WIP1. The expression of WIP1 is induced by genotoxic stress and in a negative feedback loop it efficiently inhibits p53. Thus, MDM2 and WIP1 can act on the same pathway creating the rationale to use their inhibitors together in cancer therapy.
Promising effects of the combination with MDM2 inhibitors and WIP1 inhibitors obtained in many preclinical studies using solid tumors cells pave the way to their application also in AML [66,77,78]. GSK2830371 is an active allosteric WIP1 inhibitor, selective for Wip1 with an IC50 of 6 nM against WIP1 compared to >10 μM IC50 for PPM1A & PPM1K, and >30 μM IC50 for 22 other phosphatases tested. GSK2830371 is believed to interact with the flap subdomain located near the Wip1 catalytic site, a feature that distinguishes Wip1 from other members of the protein phosphatase 2C (PP2C) family.
In osteosarcoma and neuroblastoma cells WIP1 accentuates the phosphorylation of p53 in response to MDM2 inhibitor, potentiating apoptotic and growth inhibitory response to nutlins in *TP53* wild-type cells, particularly in those with high *PPM1D* expression or activity [79]. Therefore, these evidences demonstrate the enhanced p53 transcriptional activity in response to the combination of MDM2 inhibitors and GSK2830371, as it is enhanced also p53 mediated growth inhibitory and apoptotic response. In fact, all changes in the cell cycle regulation mediated by MDM2 inhibitors were incentivized by the association with WIP1 inhibitor, for example G1:S and G2:S were significant in

the presence of GSK2830371[79]. Also in breast cancer the simultaneous inhibition of WIP1 and MDM2 to restore p53 pathway increased the percentage of apoptotic blast cells and sensitizing them to doxorubicin[80].

Moreover, a study showed that GSK2830371 at doses with no growth-inhibitory activity alone, potentiated the growth-inhibitory and cytotoxic activity of MDM2 inhibitors by increasing phosphorylation, acetylation and stabilization of p53 in cutaneous melanoma cells in a functional p53-dependent manner.[77] Finally, a recent paper showed that also in AML WIP1 could be an important target, in fact J. Kahn et al. demonstrated that truncating *PPM1D* mutations confer chemotherapy resistance, leading to the selective expansion of *PPM1D*-mutant cells in vitro and in vivo and that WIP1 treatment reverses the chemotherapy resistance phenotype (to cytarabine) and selectively kills *PPM1D*-mutant cells (**Figure i6**). [1]

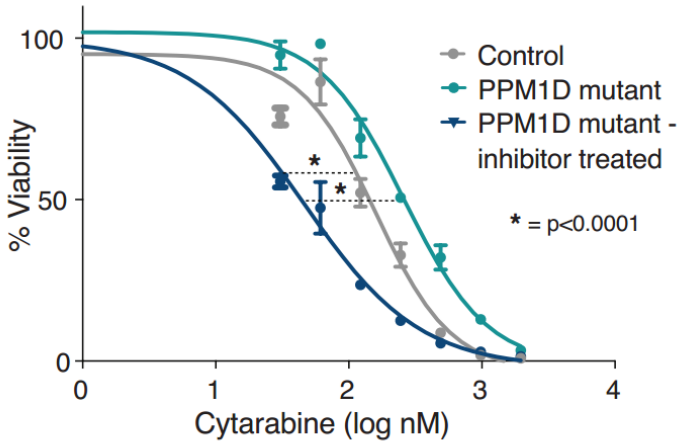

Figure i6. *PPM1D* inhibition with GSK2830371 reverses chemotherapy resistance and selectively targets *PPM1D*-mutant cells: 72h Viability analysis of MOLM-13 *PPM1D*-mutant cells vs MOLM-13 control single cell clones pre-treated for 1 hour with 3μM GSK2830371 or vehicle and exposed to increasing doses of 72-hour cytarabine treatment.[1]

Currently, it is possible to affirm that pharmacological inhibition of WIP1 combined with MDM2 inhibitors is a promising therapeutic strategy in *TP53*-wt cancers and that *PPM1D* mutational status, even if quite rare mutated in AML, could be considered as a predictive biomarker for response to this combination treatment.

AIM OF THE THESIS

Defining the genomic abnormalities and profiles that are responsible for poor prognosis in AML is still a need. The advent of powerful high-resolution technologies for patient characterization (such as genomics, proteomics and multidrug response assays) has dramatically improved the knowledge of hematological malignancies. Moreover, these approaches allowed the identification of potential oncogenes related to drug-resistance and new mechanisms of genomic instability associated with poor prognosis and early relapse rate.

The main aim of this thesis was to deeply characterize the pathogenic mechanisms of dysfunction in the p53 pathway in AML, by analyzing genomic instability mechanisms (chromothripsis) and resistance to drugs currently used in clinical practice, in order to define new targets and biomarker of response.

Since *TP53* is a target of both genomic and functional inactivation in AML, we focused our studies on the effects of mutant *TP53* (chromothripsis-related) and on the mechanisms underlying non-mutational p53 inactivation (the activity of WIP1 and MDM2 proteins in the regulation of p53 functions). The results of the present work might be of therapeutic relevance, leading to tailored and rationalized p53-based therapy in the era of precision medicine.

RESULTS

Chromothripsis in Acute Myeloid Leukemia: biological features and impact on survival

Maria Chiara Fontana[1], Giovanni Marconi[1]*, Jelena D. Milosevic Feenstra[2], Eugenio Fonzi[1], Cristina Papayannidis[1], Andrea Ghelli Luserna di Rorá[1], Antonella Padella[1], Vincenza Solli[1], Eugenia Franchini[1], Emanuela Ottaviani[1], Anna Ferrari[1], Carmen Baldazzi[1], Nicoletta Testoni[1], Ilaria Iacobucci[1,3], Simona Soverini[1], Torsten Haferlach[4], Viviana Guadagnuolo[1], Lukas Semerad[6], Michael Doubek[6], Michael Steurer[7], Zdenek Racil[6], Stefania Paolini[1], Marco Manfrini[1], Michele Cavo[1], Giorgia Simonetti[1&], Robert Kralovics[2&] and Giovanni Martinelli[1&].*

[1] Institute of Hematology "L. and A. Seràgnoli", University of Bologna, Italy
[2] CeMM Research Center for Molecular Medicine of the Austrian Academy of Sciences, Wien, Austria
[3] Present: Department of Pathology, St. Jude Children's Research Hospital, Memphis, TN, USA
[4] MLL Munich Leukemia Laboratory, Munich, Germany
[6] Department of Internal Medicine - Hematology and Oncology, Masaryk University and Hospital, Brno, CR
[7] Division of Hematology and Oncology, Medical University of Innsbruck, Innsbruck, Austria

Leukemia. 2018 Jul;32(7):1609-1620. doi: 10.1038/s41375-018-0035-y.

INTRODUCTION

Loss of chromosomes and complex karyotype are mechanisms of genomic instability known to be linked to therapy resistance, poor prognosis and early relapse in AML[7,81,82]. Nowadays, new high-throughput technologies can discover new alterations responsible for the poor prognosis in sub-cohorts of AML patients and may reveal druggable pathways. There is an urgent need to define genomic phenotypes in AML in a prognostic and therapeutic perspective.

Chromothripsis is a one-step genomic catastrophe involving one or few chromosomes resulting from chromosome breakage and random DNA rejoining[83]. It has been detected, mainly as occasional finding, in solid tumors[43–51] and hematological malignancies (multiple myeloma[52], AML[53,54], acute lymphoblastic leukemia[55,56], chronic lymphocytic leukemia[57]), as well as in germline cases of congenital disorders[58]. A study on 22,000 cases of primary tumors highlighted an overall incidence of chromothripsis between 2% and 3%[84].

During mitosis, chromothripsis arises from aberrant DNA replication timing. Prolonged arrest of cell cycle and micronuclei formation influence the spatial distribution of damages favoring the acquisition of structural rearrangements[85]. Molecular mechanisms implicated in this event are only partially discovered. Chaotic genomes seemed to form through random non-homologous end joining after DNA damages[86]. An alternative theory presented chromothripsis as a putative incomplete outcome of chromosome fragmentation, the initial event triggering a new form of mitotic cell death[86]. Moreover, recent evidence indicates that chromothripsis preferentially occurs especially in hyperploid cells[87] and in cells with damaged telomeres[88]. Chromothripsis has been associated to

EGFR, *MDM2* and *MDM4* amplification, *CDKN2A* and *PTEN* deletion[46], aberrant DNA double-strand break (DSB) response[89], *TP53* mutations[47,53], complex karyotype[47,53] and with *ATM* mutation[56]. Analysis of additional tumor entities substantiates a link between *TP53* mutation and chromothripsis, and indicates a context-specific role for p53 in catastrophic DNA rearrangements. [47]
At present, a standardized way to detect chromothripsis does not exists, but a few have been proposed. Chromothripsis has been identified with fluorescent in situ hybridization (FISH) [47,53,54,89], or, alternatively, by operator-dependent analyses[52] as well as algorithm-based detection of shattering patterns on SNP array data and eventual integration with DNA sequencing data[84,90]. Korbel and Campbell defined six different criteria to distinguish chromothripsis from a multi-step process of genomic rearrangement[91]. When analyzed by SNP arrays, chromosomes harboring chromothripsis show a characteristic pattern of alterations: two or three switches of CN state detectable along the chromosome with a clustering of breakpoint locations[92]. These patterns are associated with a high number of chromosomal rearrangements (tens to hundreds) with widespread loss or gain of sequence fragments interspersed in diploid regions[84].
Chromothripsis has been associated with highly aggressive disease in various tumors[46–52]. However, it did not appear to impact prognosis, both in term of therapy response and overall survival (OS), in prostate cancer[93] and in estrogen receptor-negative breast cancer[50]. [59]

METHODS

Patients

Samples and data at diagnosis from 395 adult patients affected by *de novo* or secondary AML according to WHO 2016 criteria[9] were collected from 3 Institutions: 1) the Department of Experimental, Diagnostic and the Specialty Medicine of University of Bologna (Italy, n = 121) in Italy, 2) the Research Center for Molecular Medicine (CeMM) of the Austrian Academy of Sciences (n = 161, of which 98 were previously published[94,95], genomic data not released) for samples from Austria, Czech Republic, and Serbia and 3) the University of Michigan (US, n = 114, all previously published[62], GSE23452). Samples with acute promyelocytic leukemia were excluded. The study was approved by the local ethical committees and written permission and informed consent were obtained from all patients before sample collection according to Helsinki declaration of "Ethical Principles for Medical Research Involving Human Subjects"[96].
Data were collected and managed through custom Electronic Case Report Forms using REDCap electronic data capture tool[97] hosted at Istituto Seràgnoli (Department of Experimental Diagnostic and Specialty Medicine, University of Bologna, Italy).

Cells and DNA isolation

Pre-treatment bone marrow and/or peripheral blood cells were processed by Ficoll-Hypaque. DNA was extracted using AllPrep DNA/RNA MiniKit (QIAGEN) in accordance with manufacturer's instructions. DNA quality and quantity were assessed using the NanoDrop Spectrophotometer (NanoDrop Technologies).

Samples from CeMM and University of Michigan were processed as previously described[62,94,95].

SNP microarray analysis

DNA samples were processed by Affymetrix® Genome-Wide Human SNP 6.0 (n = 321) and Cytoscan HD Array (n = 84) according to manufacturer's instructions. Of the 114 SNP 6.0 AML cases obtained from GSE23452, 112 were paired samples, including buccal swab DNA or bone marrow at remission[62]. Array data have been deposited in the NGS-PTL repository (http://www.ngs-ptl.com/documents/documents/3-10-en/media.aspx).

Affymetrix CEL files were analyzed using Genotyping Console (Affymetrix®) and Chromosome Analysis Suite (ChAS, Affymetrix®) for initial quality control of Median Absolute Pairwise Difference (MAPD); we collected all the samples that had a median of 0.25 for Cytoscan HD Array and 0.35 for SNP Array 6.0. MAPD mean in the entire set was 0.27, standard deviation 0.05, variance 0.003. CN alterations (CNA), allele ratio, and allele specific CN data analyses were performed on CEL files using Nexus CN software v. 8.0 (BioDiscovery).

For non-paired samples (n = 283), CNA were filtered against a pool of 291 healthy individuals from Ontario Population Genomics Platform performed by Cytoscan HD Array[98] and on the Database of Genomic Variants (DGV, website).

Detection of chromothripsis

Chromothripsis was defined according to Korbel and Campbell's criteria[91], when 3 out of 6 criteria were satisfied (the remaining criteria could not be assessed by SNP array analysis).

Chromothripsis, as described above, was assessed by scanning SNP array segment files using *CTLP*-Scanner (using R v3.3.2[99] and "*CTLP* scanner" package[84]). The following thresholds were set: Log Ratio ≥ 8, more than 10 breakpoints, minimum segment size of 10 kb, and 0.3 as signal distance between adjacent segments. Events with a prevalent CN status and CN status changes involving $\leq$ 10% of detected region were excluded.

Chromothripsis events were then confirmed by visual inspection using both Nexus CN Software v. 8.0 (BioDiscovery) and R package "Rawcopy" [100], in order to verify the presence of a CN-LOH in

the B-allele frequency (BAF), to assess technical quality (hybridization level and quality of the physical array) and to obtain an extensive overview of chromosomal aberrations.

Microarray statistical analyses

CEL file reports were exported from Nexus CN (BioDiscovery) v. 8.0 and went through statistical analysis using R v3.3.2[99] and Bioconductor v3.4 (BiocInstaller 1.24.0) with following packages: "org.Hs.eg.db" v3.4.0[101], "reactome.db" v1.58.0[102], "clusterProfiler" v3.2.11[103], "ReactomePA" v1.18.1[104]

Based on the presence/absence of chromothripsis, AML samples were divided in two groups: a group of cases (patients with chromothripsis) and a group of controls (patients without chromothripsis) and enrichment of CNA events between the two groups was examined. The dataset was stratified for event type and the statistical tests were performed on the following event groups: amplifications of one or more DNA copies, and heterozygous or homozygous deletions. In each patient, multiple events of the same type in the same gene were considered as one. All p-values were adjusted for multiple testing with Benjamini-Hochberg method[105]. Fisher's exact test was used to compare frequencies in genes' event between two groups. Genes which are not reported in Atlas of Genetics and Cytogenetics in Oncology and Haematology[106] and which did not contain at least one event at single gene's level with an adjusted p-value lower than 10^{-4} in the Fisher exact test comparison were filtered out. For testing at a pathway level, genes were annotated in the Reactome database[107]. Firstly, pathway enrichment analysis was performed at patient level by means of an over-representation test (based on hypergeometric distribution)[103]. Then, the adjusted p-values obtained for a certain pathway across all patients were used as predictor variable in a logistic regression model fitted against the case/control classification as dependent variable (0 = case, 1 = control, ctrl); p-values from all the performed logistic regression tests were in turn adjusted for multiple testing. The significance level was set at 10^{-4} (adj-p < 10^{-4}; CI 99.9999%).

Molecular analyses

The mutational status of exons 5-9 of *TP53*, exon 12 of *NPM1*, exons 13-15 and 20 of *FLT3* was determined using specific primers for qualitative PCR. Mutated samples where then confirmed by Sanger sequencing, using the same PCR primers. *CEBPA*, *IDH1*, *IDH2* and *TP53* mutations were directly investigated by PCR and Sanger sequencing. Presence of *FLT3*-tyrosine kinase domain (TKD) mutations was determined by digestion with specific restriction enzymes (Promega), for the detection of *FLT3*-internal tandem duplication (ITD), insertions in *NPM1* and *DNMT3A* mutations, a

denaturing high performance liquid chromatography screening (D-HPLC; Transgenomic) was done, followed by direct Sequencing of D-HPLC-positive samples. The expression of WT1 was quantified with a Real Time PCR assay (Ipsogen WT1 ProfileQuant Kit) using *ABL* as control gene (sensitivity 10^{-4}). In the group of samples from CEMM and University of Michigan, the mutational status of the same genes described above plus *RUNX1, CBL, NRAS* were assessed as previously described[62,94,95].

Chromosome Banding Analysis

CBA was performed on bone marrow cells after short-term cultures (24 and/or 48 h). Briefly, the cells were treated with colchicine and hypotonic solution and the pellet was fixed and washed in methanol/acetic acid (3:1). The cells were then re-suspended in fixative and dropped on slides. Karyotypes were examined after G banding technique and described according to International System for Human Cytogenetic Nomenclature (ISCN 2016)[108]. Complex karyotype was defined as three or more chromosomal abnormalities in the same clone.

FISH

FISH analysis was carried out on previously G-banded metaphases prepared by CBA technique according to manufacturer's instructions. To characterize the chromosomes involved in chromothripsis, we used whole chromosome painting probes specific for chromosomes 5 and 12, (Kreatech, Leica Biosystem,Wetzlar, Germany), LSI *MYC* Dual Color, Break Apart Rearrangement Probe (Vysis, Abbott Molecular, IL, USA), LSI *MLL* Dual Color, Break Apart Rearrangement Probe (Vysis) *CEP17* Spectrum Green/LSI *TP53* Spectrum Orange (Vysis), *EVI1* (MECOM) Tricolor Breakapart Probe (Cytocell, Cambridge, UK). The slides were counterstained with DAPI and analyzed using fluorescent microscopes equipped with FITC/TRITC/AQUA/DAPI filter sets and the Genikon imaging system software (Nikon Instruments, Tokyo, Japan).

Clinical Statistical analysis

Clinical data collection included age at diagnosis, de novo/secondary AML, White Blood Cells (WBC) count at diagnosis, therapy information (induction therapy, response to induction, consolidation courses), Hematopoietic Stem Cell Transplant (HSCT), death or last follow-up date, cytogenetic data at diagnosis, molecular data (mutations of *TP53, FLT3, NPM1, IDH1, IDH2, DNMT3A, CEBPA, RUNX1, CBL, nRAS, WT1* expression*)* at diagnosis. Due to the data-pool feature of our set, missing data will be detailed in the result section. OS was assessed as the time in days from diagnosis to death or last follow-up.

Fisher's exact test and chi-squared test were used for crosstabs and difference between distributions was assessed with median test for independent samples and Mann-Whitney U test. Logistic regression models were applied to identify putative risk factors. Survival analyses were carried out with Kaplan-Meier method[109] and significance was assessed by Log Rank test [110]. Regression models were built based on Cox Hazard Ratio[111]. Analyses and graphs were obtained with IBM SPSS Statistics 20®.

RESULTS

Clinical and molecular patient characteristics

All patients' clinical and molecular characteristics are listed in Table 1, missing data are quantified in Table S1. In our cohort, 26 out of 395 patients (6.6%) showed chromothripsis involving different chromosomes.

Table 1: clinical and molecular characteristics of the patients enrolled in this study (N = 395)

Parameter	Value
Age	Median 59.35 (range 16-92)
Sex	185/395 patients were female (46.8%) 210/395 patients were male (53.2%)
***De novo* AML**	307/372 patients (82.5%)
AML secondary to myelodysplastic syndrome	43/372 patients (11.6%)
AML secondary to other myeloid neoplasms	4/372 patients (1.1%)
Therapy related AML	18/372 patients (4.8%)
WBC (mean)	28.140/mm^3 (100-171.00/mm^3)
WBC count greater than 30,000/mm^3	46/154 patients (29.9%)
WBC count greater than 100,000/mm^3	12/154 patients (7.8%)
European Leukemia Net (ELN) Low Risk [112]	35/352 patients (8.9)%
European Leukemia Net (ELN) Intermediate 1 Risk [112]	100/352 patients (28.4%)
European Leukemia Net (ELN) Intermediate 2 Risk [112]	80/352 patients (22.7%)
European Leukemia Net (ELN) High Risk [112]	137/352 patients (38.9%)
Chemotherapy in induction ***Gemtuzumab Ozagomicin was added*** ***Complete remission***	251/308 patients (81.5%) *42/251* patients *(16.7%)* *153/251* patients *(60.9%)*
Hematopoietic Stem Cell Transplant	85/283 patients (30.0%)
Loss or a mutation of TP53 at diagnosis ***loss*** ***mutation***	63/395 patients (15.9%) 29/395 patients (7.3%) 53/324 patients (16.4%)
Internal tandem duplication in *FLT3*	42/298 patients (14.1%)
Tyrosine kinase domain mutation in *FLT3*	18/298 patients (6.0%)
Mutations in *NPM1* gene	50/286 patients (17.5%)
Mutations in *IDH1* gene	4/121 patients (3.3%)
Mutations in *IDH2* gene	11/135 patients (8.3%)
Mutations in *DNMT3A* gene	7/38 patients (19.4%)
Mutations in *CEBPA* gene	5/106 patients (4.7%)
Mutations in *RUNX1* gene	11/87 patients (12.6%)
Mutations in *CBL* gene	2/91 patients (2.2%)
Mutations in NRAS gene	10/95 patients (10.5%)

Correlation of chromothripsis with clinical and molecular parameters in AML patients

Patients showing chromothripsis were older compared to patients without chromothripsis, with a median age of 67 and 60 years, respectively (p = .002, Figure S1 C) and had a significantly lower WBC count mean at diagnosis, 6342/mm^3 *vs* 30,059 respectively (p = .040, Figure S 1A). Chromothripsis-positive AML patients presented a prevalence of complex karyotype and were classified as HR disease according to ELN definition (p < .001, Figure S 1D).

Based on genetic features, chromothripsis was associated with *TP53* loss (p < .001) and *TP53* mutations (p < .001). Only 3/26 patients did not harbor any *TP53* alteration; in 2/26 patients we did not test *TP53* mutation because of unavailable material at diagnosis, and no 17p loss was detectable; 1/ 26 patient was negative for *TP53* mutations and did not have evidence of 17p loss. Chromothripsis was mutually exclusive with *FLT3* (Figure S 1B, p = .025) and *NPM1* mutations (p = .032). Associations with other parameters is detailed in Table 2.

Table 2: correlation of chromothripsis with clinical data in 395 AML patients. (abbreviations: mut, mutated; TKD, tyrosine kinase domain; ITD, internal tandem duplication).

Parameters	Patient with chromothripsis	Patient without chromothripsis	Test	P	Significance
Age at diagnosis (median, years)	67 (range 58-85)	60 (range 16-92)	Median test	.002	**
WBC count at diagnosis (mean)	6342/mm^3 (range 1420-26700)	30.059/mm^3 (range100-171.000)	Man Whitney U	.040	*
ELN risk [113]	26/26 patients (100%) HR	35/326 patients (10.7%) LR; 100/326 patients (31.2%) INT-1; 20/326 patients (24.5%) INT-2; 111/326 patients (34.0%) HR.	χ^2	< .001	***
Median Absolute Pairwise Difference (MAPD)	.19	.28	Median test	.270	ns
***WT1*/10.000 *ABL* (median)**	8.400 (range 20-120.111)	9.200 (range 6-140.131)	Median test	1.000	ns
***FLT3* status**	0/21 patients (0%) with *FLT3* alterations	43/277 patients (15.5%) *FLT3* ITD; 18/277 patients (6.5%) *FLT3* TKD	χ^2	.025	*
***TP53* loss**	9/26 patients (34.5%)	25/344 patients (6.8%)	Fisher's exact test	<.001	***
***TP53* mut**	22/24 patients (84.6 %)	31/300 patients (10.3%)	Fisher's exact test	<.001	***
Secondary AML (every neoplasm)	6/23 patients (26.1%)	59/349 patients (16.9%)	Fisher's exact test	.196	ns
***NPM1* mut**	0/21 patients (0%)	50/263 patients (19%)	Fisher's exact test	0.032	*
***IDH1* mut**	0/7 patients (0%)	4/109 patients (3.5%)	Fisher's exact test	.784	ns
***IDH2* mut**	0/9 patients (0%)	10/125 patients (8.0%)	Fisher's exact test	.486	ns
***DNMT3A* mut**	1/5 patients (20%)	6/31 patients (19.4%)	Fisher's exact test	.685	ns
***CEBPA* mut**	0/4 patients (0%)	5/102 patients (1.4%)	Fisher's exact test	.822	ns

***RUNX1* mut**	1/3 patients (33.3%)	10/84 patients (11.9%)	Fisher's exact test	.337	ns
***NRAS* mut**	0/6 patients (0%)	10/89 patients (11.2%)	Fisher's exact test	.503	ns

Chromothripsis defined a group of AML patients with poor prognosis

Patients were treated as shown in Table 3. At induction, patients with chromothripsis were treated with intensive chemotherapy in a smaller proportion, if compared with patients without chromothripsis (p = .003). There was no difference in use of Gemtuzumab Ozagomicin during induction between the two group of patients (p=1.000) and there was a similar transplant rate between the two groups (21% of patients with chromothripsis and 31% of patients without chromothripsis received HSCT, p = .448). Chromothripsis defined a group of patients with poor prognosis. Three out of 10 patients with chromothripsis (30%) responded to induction, a significant lower proportion if compared with 152/229 patients without chromothripsis (66.4%, p = .036). In our set, a logistic regression model based on age at diagnosis, *FLT3* status, *NPM1* mutation, *TP53* mutation and chromothripsis suggested that only *TP53* mutation was correlated with response to induction chemotherapy (data not shown).

Patients with chromothripsis showed a worse OS (median OS of 120 days compared to 494 days for patients without chromothripsis, p < .001, Figure 1A). In patients with available HSCT data, this difference was confirmed by censoring OS at HSCT with a median OS of 120 and 400 days in the two groups (p < .001, Figure 1B). Patients with chromothripsis had the worst prognosis among patients with HR features according ELN2017[7] risk stratification (median OS of 120 and 258 days in the two groups, p = .011, Figure 1C). This observation was confirmed when censoring OS at HSCT (median OS of 120 and 211 days in the two groups, p = .022, Figure 1D). Moreover, the impact of chromothripsis on OS was evaluated in patients with HR features according ELN2017[7] risk stratification, who received induction chemotherapy. We report a difference in survival between patients with and without chromothripsis (median OS of 120 and 295 days respectively, p = .040, Figure 1E) and a trend towards statistical significance in HSCT-censored analysis (median OS of 120 and 242 days respectively, p = .055, Figure 1F). Patients with chromothripsis did not show survival differences compared to patients harboring *TP53* mutation, due to the high co-occurrence of these two phenomena. However, in our set patients with chromothripsis showed a survival disadvantage near to the statistical significance threshold when compared with patients with *TP53* loss (data not showed, p=.049). We built a prognostic model using COX HR with forward conditional method, considering chromothripsis event, secondary AML, ELN 2017 risk, induction therapy, *FLT3* and *NPM1* mutation as categorical variables and age at diagnosis. *TP53* status was not included in the

model for the high co-occurrence of chromothripsis and *TP53* alterations. In the optimal model, chromothripsis (HR 2.286, 95% CI 1.327-3.940, p=.003) and secondary disease were associated with augmented risk of death, while ELN2017 low risk, intermediate 1 and intermediate 2 risk were associated with better outcome (Figure 2). Chromothripsis was a consistent risk factor in COX HR model built in ELN 2017 HR population considering chromothripsis, secondary AML, induction therapy, *FLT3* mutation and *NPM1* mutation as categorical variables, and age of diagnosis (HR 2.070, 95% CI 1.167-3.672, p=.013, model not shown).

Chromothripsis was also a consistent risk factor in COX HR model built in ELN2017 HR population treated with intensive therapies considering chromothripsis, secondary AML, *FLT3* mutation, and *NPM1* mutation as categorical variables, and age of diagnosis (HR 2.227, 95% CI 1.022-4.850, p=.044, model not shown, model not shown).

Figure 1

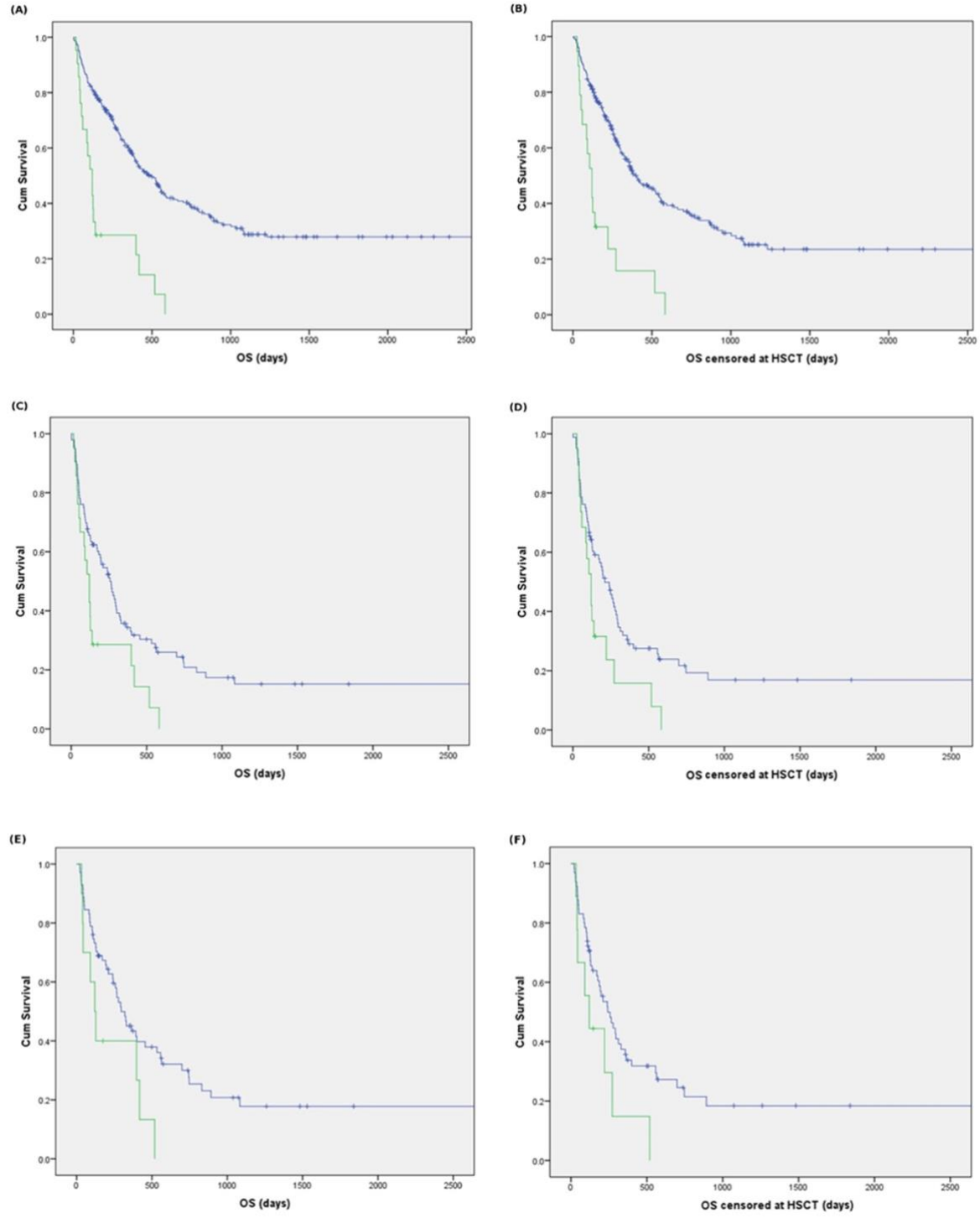

Figure 1: Association between chromothripsis and OS in AML

OS in patients with (green line) and without chromothripsis (blue line): panel (A) overall cohort, panel (B) survival censored at HSCT; panel (C) patients with ELN[112] HR features; panel (D) patients with ELN[112] HR features censoring survival at HSCT; panel (E) patients treated with intensive chemotherapy with ELN 2017 HR features; panel (F) patients treated with intensive chemotherapy with ELN[112] HR features censoring survival at HSCT.

Figure 2

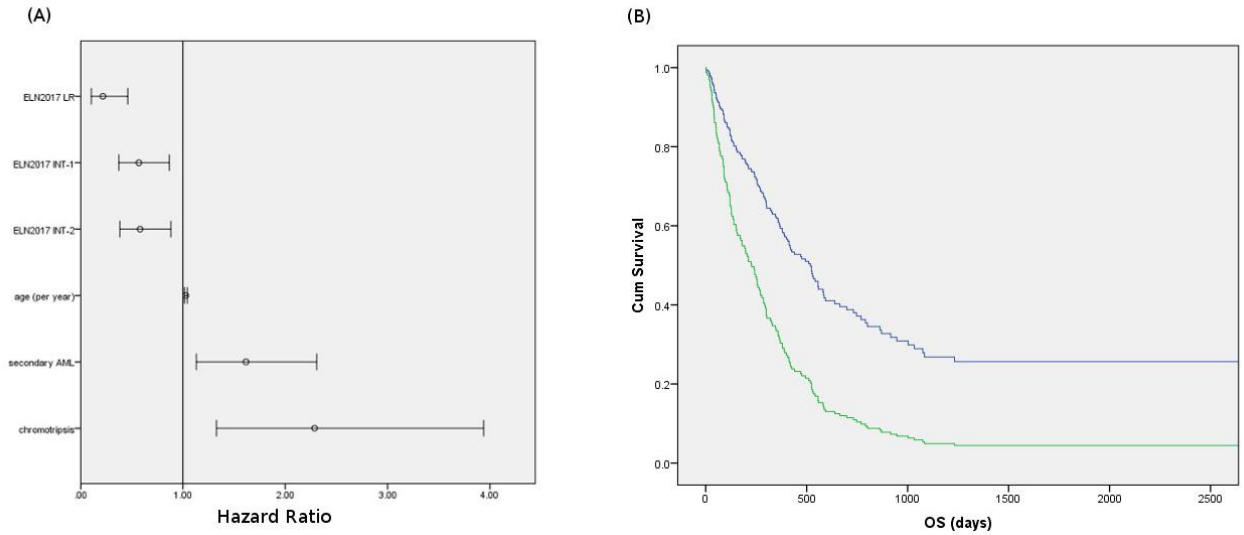

Figure 2: COX-HR model

COX-HR model in patients' set considering (A) forest plot of risk factors in COX-HR optimal model (B) in COX-HR model, difference in OS (OS) representing population with (green line) and without (blue line) chromothripsis.

Table 3: Induction therapies in patients with and without chromothripsis

Induction therapy	Chromothripsis	
	No (288)	Yes (20)
Chemotherapy – n.	241	10
Hypomethylating agents – n.	23	4
Best supportive therapy – n.	24	6

Genomic characteristics of AML patients with chromothripsis

We detected chromothripsis on chromosome 12 (23% of events), 17 and 5 (17% of events both), chromosomes 6 (10% of events), 3 and 8 (6.6% of events both), 7, 10, 11, 15, 20 (3.3% of events each) (Fig. 3, Fig. S2). SNP array analyses showed that chromothripsis-positive patients were characterized by a high grade of genomic aberrations.

We found a minimal common deleted region in 24/26 patients with chromothripsis (5q31.1-5q33.1). Among chromothripsis-negative patients, 51/369 harbored at least a CNA of 9 Mb in the 5q arm. There was a higher incidence in macroscopic deletions on 5q in patients with chromothripsis ($p<.0001$).

Patients with chromothripsis presented higher mean of CNA than patients without chromothripsis (mean of 418 vs 188 CNA per patient; Figure 4, CIRCOS[114] external level).

Fisher Exact Test showed that a large group of 1359 genes were significantly altered in deletion (both heterozygous and homozygous) in chromothripsis-positive patients rather than chromothripsis-negative ones (data not shown). These genes map on chromosome 5q, 3q, 12p, 3p, 4q, 7q, 12p, 16q and 17p. Considering chromosome position of genes associated with chromothripsis, we found that CNA randomly affected the entire 5q and whole chromosome 3. In the other chromosomes, we found that statistically significant CNA mapped in relatively small regions (complete list of genes in Fig.4, CIRCOS[114] internal level). These regions included deletions of genes involved in Atlas of Genetics and Cytogenetics in Oncology and Haematology, in particular on chromosome 4q28-32 (*SFRP2*), 7q31.1-36.3 (*CAV1*, *EPHA1* and *NRF1*), 12p11.21-13.3 (*EPS8*, *RECQL* and *GUCY2C)*, 16q22-24.3 (transcription factors *CBFA2T3* and *FOXF1; CDT1* involved in DNA replication; and the Fanconi Anemia gene *FANCA*), and 17p13-13.1 (*ALOX12* and *CLDN7*) (Figure 4). Genes were filtered as described in Methods and we showed that 95 genes were associated with chromothripsis (complete list of genes in Fig.4, CIRCOS[114] internal level).

REACTOME enrichment of pathways are reported in Table S2 and S3. DNA repair, E2F mediated regulation of DNA replication, signaling pathways involving PI3K, phospholipid biosynthesis and metabolism, and various grow factors signaling pathways scored in the best 1% of pathways enriched for amplification events in chromothripsis. CTLA4 inhibitory signaling, synthesis of Phosphatidylinositol Phosphate (PIP) at the late endosome membrane, Fanconi Anemia pathway, genes regulating G0 and early G1 phase, pre-NOTCH transcription and translation scored in the best 1% of pathways enriched for deletion events in cases with chromothripsis. In the sub cohort of patients with *TP53* mutation/deletion, when we compared patients with chromothripsis ($n = 22$) and patients without chromothripsis ($n = 44$), we did not detect any significant difference in terms of differentially altered genes and pathways (with a significance threshold of $p < 10^{-4}$).

Figure 3

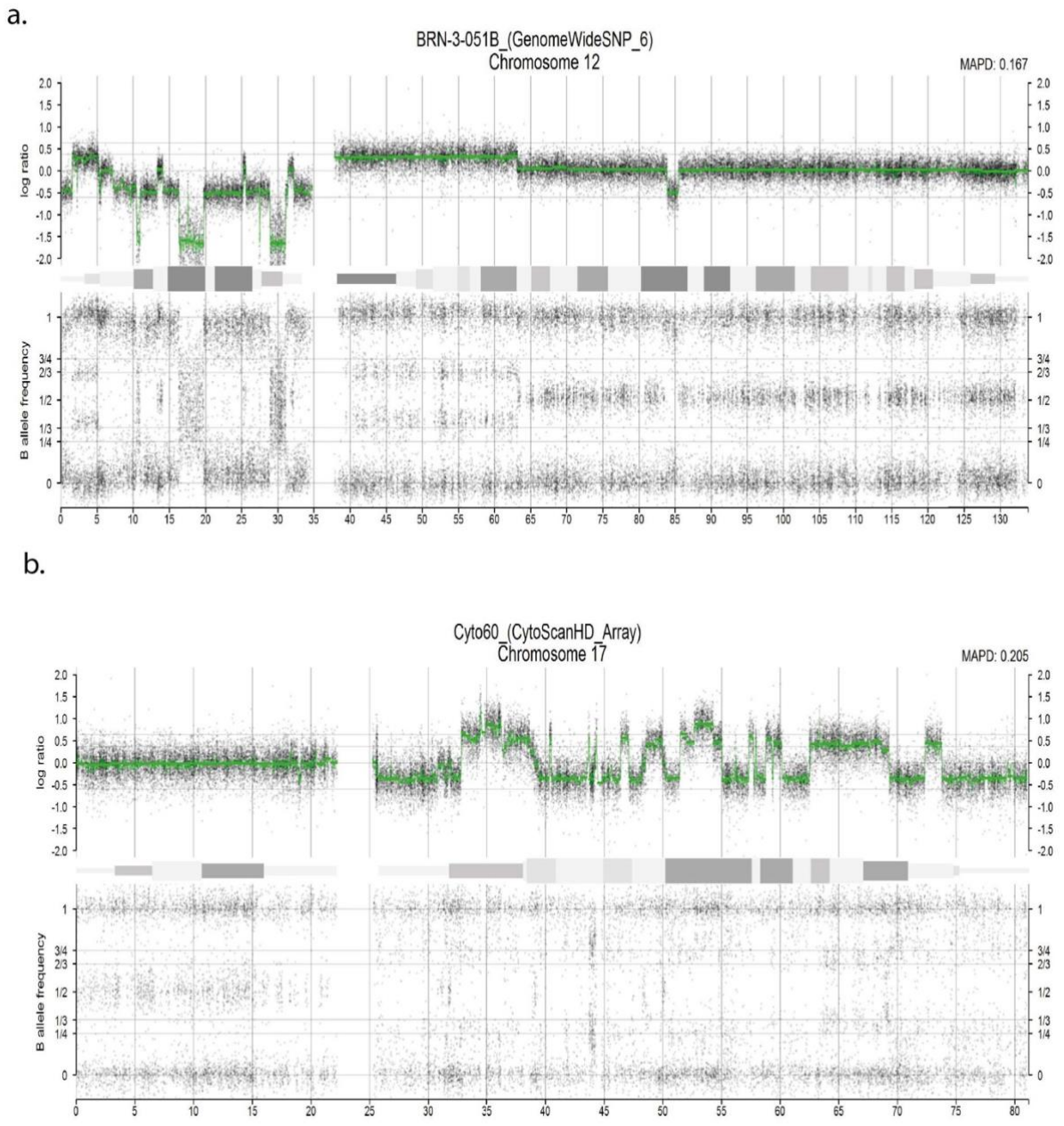

Figure 3: Representation of 2 chromosomes affected by chromothripsis in different patients, plotted with Rawcopy v. 1.0

(a) chromosome 17q with 36 switches and 2-3 changes in CN (involving also homozygous gains).
(b) chromosome 12p with 28 switches and 2-3 changes in CN (involving also homozygous losses).

Figure 4

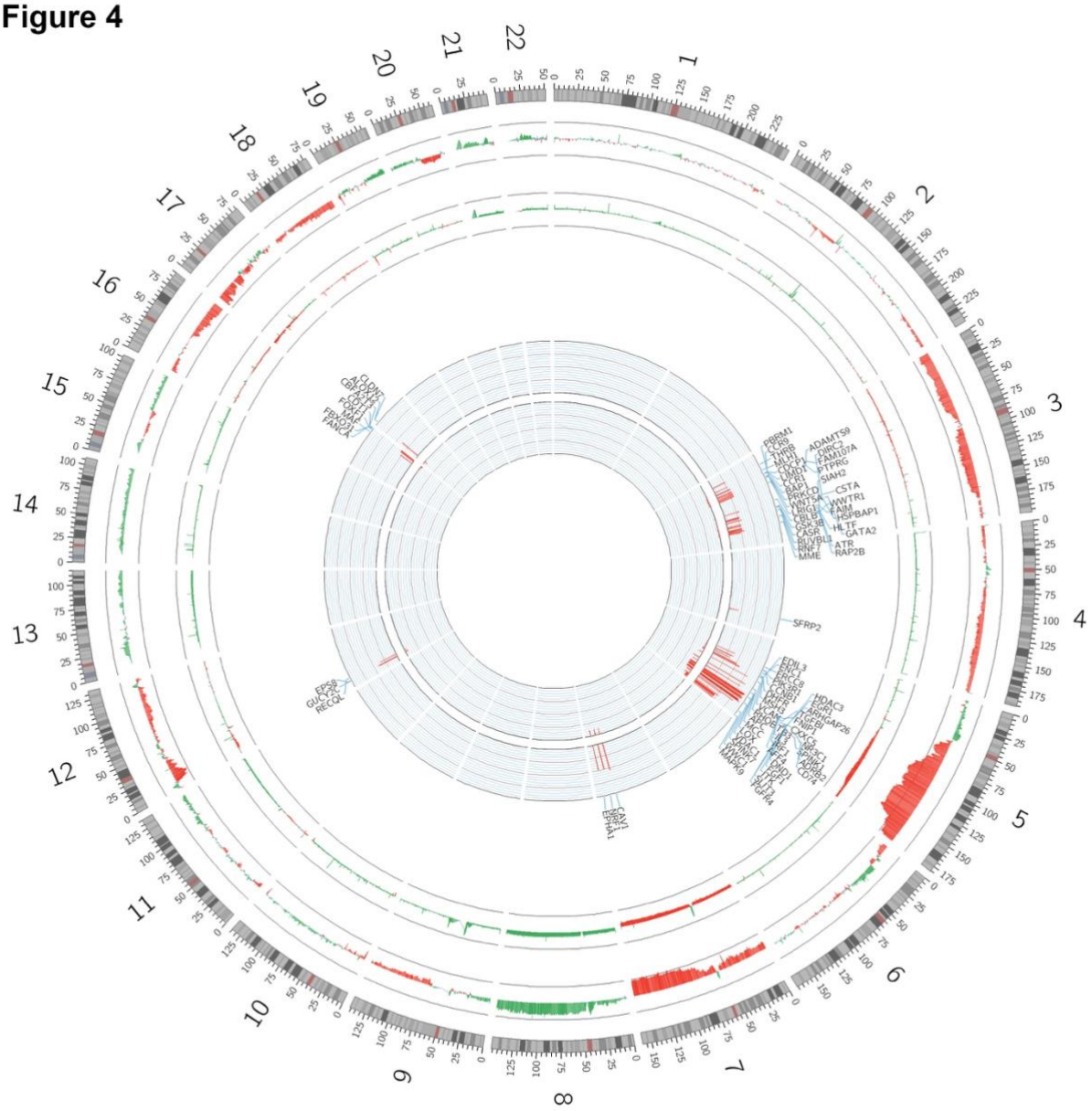

Figure 4: CIRCOS plot representing the overall CNA and genes altered in the 2 groups (chromothripsis-positive patients vs chromothripsis-negative patients)

(A) External circular level: genomic landscape in CNA per group of patients (external line represent chromothripsis-positive patients, internal line represent chromothripsis-negative patients). Green lines represent amplifications, red lines represent deletions. (B) Internal list of selected genes (basing on Fisher Exact Test and Atlas of Genetics and Cytogenetics in Oncology and Haematology) deleted in heterozygosis and/or homozygosis with relative frequency in CNA displayed with histograms: chromothripsis-positive patients (external level) and chromothripsis-negative patients (internal level).

Chromothripsis is associated with marker, derivative and ring chromosomes formation

In order to better characterize the chromosomes affected by chromothripsis, we performed FISH analysis in 7/26 cases with available material. Most cases (5/7) showed the presence of marker or ring chromosomes. In 4 cases, the chromosomes affected by chromothripsis (chromosomes 8, 11, 12 and 17) were reported by CBA as monosomic chromosomes, while, by FISH, portions of these chromosomes were identified on marker chromosomes. In cases involving chromosomes 8 and 11, the rearrangement led to amplification of MYC and *KMT2A* (MLL) genes, respectively. In cases involving chromosomes 12 and 17, parts of the chromosomes affected by chromothripsis were identified on markers and on derivative chromosomes resulting from unbalanced translocations. In other 2 cases, the chromosome involved in chromothripsis was annotated as derivative chromosome. Moreover, FISH highlighted the presence of a homogeneously staining region on the derivative chromosome 3 due to MECOM amplification in one case and of a complex translocation involving chromosome 5 in the other case. In the last patient, the chromosome affected by chromothripsis was identified as ring chromosome 17 leading to loss of *TP53*. FISH results are shown in Figure 5.

Figure 5

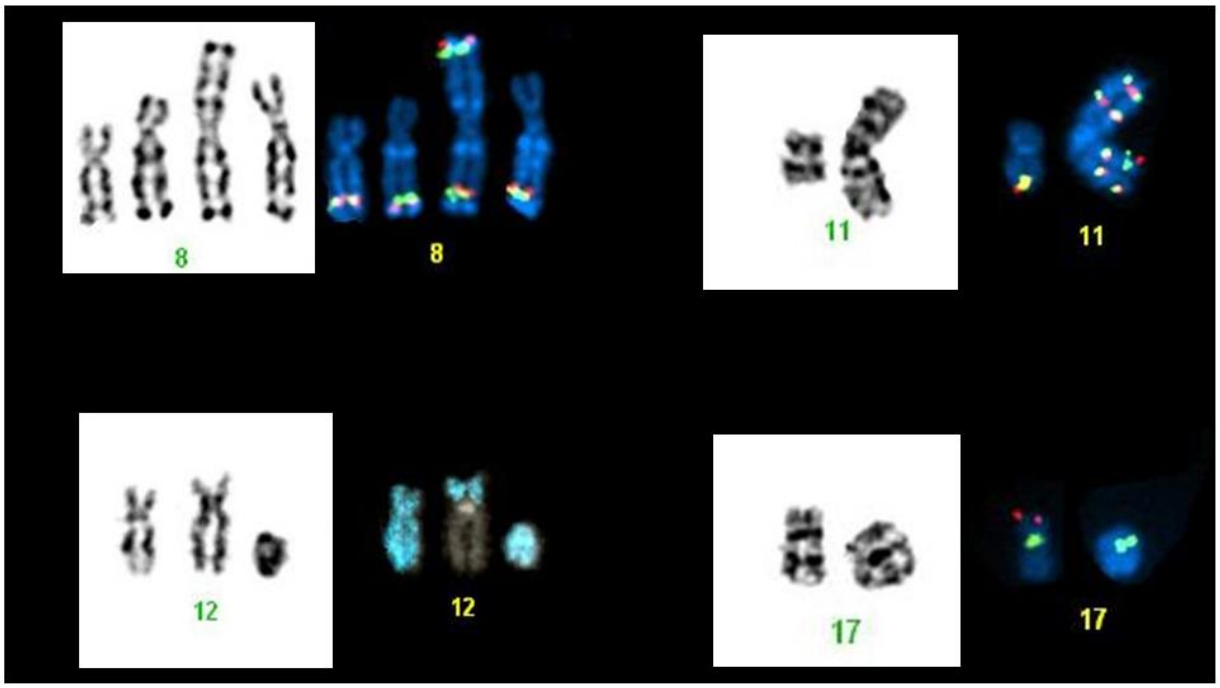

Figure 5: Karyotype analysis in AML patients harboring chromothripsis

FISH analysis with (A) MYC breakapart probe showing five fusion signals of MYC localized on normal chromosome 8 and on 3 different marker chromosomes in patient with chromothripsis of chromosome 8. (B) *KMT2A* (MLL) breakapart probe showing four copies of *KMT2A* (4 fusion signals) localized on the marker chromosome resulted from chromothripsis of chromosome 11. (C)

with whole chromosome paint probe for chromosome 12 marked in blue revealing part of chromosome 12 on the marker chromosome and on the derivative chromosome 3 from translocation t (3;12). (D) showing deletion of *TP53* gene (red signal) in the case with chromothripsis of chromosome 17 annotated as ring chromosome by CBA.

DISCUSSION

The purposes of this study were to define the incidence of chromothripsis in newly-diagnosed adult AML patients, its impact on survival and its genomic background in AML. To detect chromothripsis, we used a custom algorithm based on *CTLP* scanner[84] and Korbel and Campbell's criteria[91] that detected chromothripsis basing on SNP array data.

Our results, obtained in a large set of patients, indicate that chromothripsis is a non-anecdotal finding in AML. The overall incidence of chromothripsis was concordant with studies conducted on fewer patients[53,54]. Chromothripsis appeared to be associated with higher age and lower WBC count at diagnosis, and mutually exclusive with *FLT3* and *NPM1* mutations, these data were never reported in AL. Moreover, we confirmed the strong association between chromothripsis and *TP53* dysregulation[47,53], thus reinforcing the importance of *TP53* for the maintenance of genomic stability and integrity.

For the first time, we pointed out that the only detection of chromothripsis is sufficient to define a group of patients with poor prognosis in the general AML population and in the ELN[112] high risk population; chromothripsis was a determinant of poor OS in the COX-HR optimal model. We further performed survival analysis in the subset of patients with *TP53* alterations, as *TP53* alone was reported to define patients with the worst prognosis in AML[10,60,115] we did not detect differences in survival defined by to have or not to have chromothripsis, and this was the main limitation of our study. This may be explained by the low number of patients in this subset, the moderate number of patients with missing follow-up information, and by the slightly lower mean OS of patients with *TP53* alteration in our set when compared with literature data[115]. Furthermore, we cannot exclude that chromothripsis may be a phenotypical manifestation, or simply an epiphenomenon, of *TP53* alteration. Further tests are needed in patients' sets enriched to have *TP53* alteration or to have chromothripsis without *TP53* alteration.

Our work describes chromothripsis biological scenario basing on SNP high throughput genomic analyses; even with the limitations due to lack in availability of whole genome sequencing or gene expression data in our patients' set, we found several events significantly associated with chromothripsis. Patients with chromothripsis presented a high genomic instability, highlighted by the high number of CNA per patient and a high recurrence of losses in chromosome 3 and 5q and high incidence of complex karyotype; this result is consistent with literature[47,53,56,87,88,116–118].

Interestingly, we found in most patients with chromothripsis a minimal common deleted region in 5q31.1-5q33.1, containing key genes involved in RAS, PI3K/AKT, transcriptional factors, DNA damage, histone modification and SMAD signaling. Moreover, we found heterozygous and homozygous genes' deletions associated with chromothripsis that clustered in relatively small genomic regions. Within altered genes, we hypothesized that *FANCA* could be a candidate to cooperate at a multi-genic and multi-step mechanism that initiate and maintain chromothripsis. *FANCA* deletion is found in a relatively small genome region; furthermore it was found deleted in sporadic AML[119] and it originate a syndrome that predispose to AML. Significantly, when we performed pathway enrichment, we found DNA damage and Fanconi Anemia pathways scoring within the best 1%, together with early G0-G1 regulation, cell cycle and several other pathways that could be possibly related genesis and maintenance of chromothripsis. Tumors characterized by genetic instability and by alterations in DNA damage pathway could be the ideal target of innovative therapeutic approaches like checkpoints inhibitors[120], and combination therapies based on these agents could be an option in chromothripsis patient for patients with poor prognosis. Furthermore, our findings characterize a subset of AML patients with a high burden of alterations and potentially neoantigens, that could be the optimal candidates for novel therapies like PD1/PDL1 blocking monoclonal antibodies and immune modulating drugs, maybe in combinations with hypomethylating agents.

Compared to the subset of patients with *TP53* alteration, we did not find significant pathways and genes. This may be due to the low number of patients in this subset, and it requires further studies in enriched population with multi-omics approach.

Finally, although only a subset of cases could be analyzed by CBA and FISH, our results showed that chromothripsis was associated with marker, derivative and ring chromosomes, suggesting that these complex chromosomal rearrangements can arise from chromothripsis. This finding is in accordance with what Bochtler and colleagues previously reported[53].

In conclusion, chromothripsis is clearly a catastrophic event defining a consistent group of patients with poor prognosis which could be candidate *per se* to novel approaches; chromothripsis is associated with losses of 5q31.1-5q33.1 in most patients, and with a complex genomic background in which *FANCA, TP53* and genes regulating cell cycle seem to be fundamental and demand further pre-clinical studies.

Aknowledgments
Prof. Michele Baccarani and Prof. Michele Cavo directed Istituto Seràgnoli. Prof. Sami Nimer Malek grant access to his previously published data and give us detailed and useful information's on data organization. Robert Kralovics received funding form the Austrian Science Fund (SFB F4702). This work was supported in part by "Progetto Regione-Università 2010-12", by "FP7 NGS-PTL project (agreement n°306242-NGS-PTL)" and by HARMONY Project. The authors thank all the members of the NGS-PTL consortium and in particular Prof. Clelia Tiziana Storlazzi. The authors thank also, ELN, AIL, AIRC and PRIN.

SUPPLEMENTARY INFORMATION

Methods

SNP Array protocol

DNA from AML samples was processed through the following steps: digestion, ligation, amplification and purification, fragmentation, labeling, hybridization, washing, staining and finally scanned to obtain the CEL files, according to manufacturer's instruction. The fragmentation protocol of the group of samples performed at University of Bologna has been adjusted by increasing the volume of 10x Fragmentation Buffer and Fragmentation Reagent in order to improve the efficiency of DNA fragmented. We used an adjusted fragmentation protocol, with a bigger volume of 10x Fragmentation Buffer and Fragmentation Reagent in order to obtain a better quality of DNA fragmented, under Affymetrix Technical Support's suggestion.

Detection of chromothripsis

Chromothripsis occurred in 1 or 2 chromosomes per patient characterized by a cluster of breakpoints, regularity of oscillating CN states (2-3 CN states, e.g. from heterozygous deletions to amplifications or from heterozygous deletions to amplifications in more than one copy or to homozygous deletions) within 10 subsequent rearrangements interspersed in diploid regions and a high and variable number of breakpoints.

SNP microarray analysis

The threshold of CN gain and loss were set at 0.15 and -0.15, respectively. Copy Neutral LOH or UPD (Uniparental Disomy) was defined as a region displaying LOH without a CN loss. Chromosomic CNA of at least 1 kb and with a minimum of 8 probes per segment were considered

and sex chromosomes were excluded from genomic analysis for the lack of paired normal controls for all cases.

Microarray statistical analyses

Non-coding genes (LINC- and –IT genes), or genes considered not detectable by the limits of SNP array because involving RNA transcripts (microRNAs, small nucleolar RNAs, antisense RNAs, small cajal body-specific RNAs) or with uncertain function (LOC genes) and highly recurrent as a CN Variant (olfactory receptors, mucins, keratins, ryanodine receptors, cub and sushi multiple domain proteins, neurexins, contactins) were filtered out from the list of CNA.

Supplementary Tables

Table S1: Missing value for every parameter considered

	Valid	Missing
chromothripsis	395	0
sex	395	0
pathology	395	0
secondary	372	23
de novo	372	23
WBC > 100.000/mm^3	152	243
WBC > 30.000/mm^3	152	243
karyotype	352	43
ELN risk	352	43
induction_therapy	308	87
mylotarg in induction	274	121
induction courses	113	282
response to induction	289	106
allogenic HSCT	283	112
***TP53* loss**	395	0
MAPD	395	0
***TP53* mutation status**	324	71
***FLT3* mutation status**	298	97
***NPM1* mutation status**	286	109
***IDH1* mutation status**	121	274
***IDH2* mutation status**	135	260
***DNMT3A* mutation status**	38	357
***CEBPA* mutation status**	106	289
***RUNX1* mutation status**	87	308
***CBL* mutation status**	91	304
***NRAS* mutation status**	95	300

Table S2: best 1% scoring REACTOME pathways enriched per amplifications in one or more copy in chromothripsis patients compared with non-chromothripsis patients (sorted by score)

Pathway Super Category	Pathway Name	Altered genes/genes in the pathway	Q-VAL
Metabolism	Glycosaminoglycan metabolism	109/116	7.98E-06
Cell Cycle	E2F mediated regulation of DNA replication	26/30	2.75E-05
Disease	Constitutive Signaling by Aberrant PI3K in Cancer	58/59	2.75E-05
DNA Repair	DNA Repair	138/141	2.75E-05
Hemostasis	Platelet activation, signaling and aggregation	182/190	2.75E-05
Hemostasis	Cell surface interactions at the vascular wall	98/101	2.75E-05
Hemostasis	Tie2 Signaling	18/18	2.75E-05
Immune System	Signaling by Interleukins	99/107	2.75E-05
Immune System	Interleukin-2 signaling	38/41	2.75E-05
Immune System	Signaling by the B Cell Receptor (BCR)	184/190	2.75E-05
Immune System	Fc epsilon receptor (FCERI) signaling	162/171	2.75E-05
Immune System	CD209 (DC-SIGN) signaling	20/21	2.75E-05
Metabolism	Glycerophospholipid biosynthesis	87/90	2.75E-05
Metabolism	Phospholipid metabolism	133/139	2.75E-05
Signal Transduction	SOS-mediated signalling	14/14	2.75E-05
Signal Transduction	Signaling by EGFR	164/168	2.75E-05
Signal Transduction	Signalling to ERKs	37/37	2.75E-05
Signal Transduction	Signaling by FGFR	148/151	2.75E-05
Signal Transduction	Signaling by ERBB4	141/143	2.75E-05
Signal Transduction	Signaling by Leptin	21/21	2.75E-05
Signal Transduction	Signaling by FGFR1	148/151	2.75E-05
Signal Transduction	Signaling by FGFR2	148/151	2.75E-05
Signal Transduction	Signaling by FGFR3	148/151	2.75E-05
Signal Transduction	Signaling by FGFR4	148/151	2.75E-05
Signal Transduction	RHO GTPases Activate Formins	94/102	2.75E-05
Transmembrane transport of small molecules	Ion channel transport	159/177	2.75E-05

Table S3: best 1% scoring REACTOME pathways enriched per heterozygous and homozygous deletions in chromothripsis patients compared with non chromothripsis patients (sorted by score)

Pathway Super Category	Pathway Name	Altered genes/genes in the pathway	Q-VAL
Immune System	CTLA4 inhibitory signaling	9/11	6.95E-13
Immune System	CLEC7A (Dectin-1) induces NFAT activation	10/12	6.95E-13
Metabolism	Synthesis of PIPs at the late endosome membrane	9/10	6.95E-13
Fanconi Anemia pathway	Fanconi Anemia pathway	19/24	1.30E-12
Metabolism	alpha-linolenic (omega3) and linoleic (omega6) acid metabolism	8/13	1.30E-12
Metabolism	alpha-linolenic acid (ALA) metabolism	8/13	1.30E-12
Metabolism of proteins	Calnexin/calreticulin cycle	10/11	1.42E-12
Cell Cycle	G0 and Early G1	19/21	1.47E-12
Disease	Diseases of metabolism	30/35	1.47E-12
Extracellular matrix organization	Laminin interactions	24/30	1.47E-12
Immune System	Growth hormone receptor signaling	21/23	1.47E-12
Metabolism	Heme biosynthesis	07/11	1.47E-12
Metabolism	Synthesis of bile acids and bile salts via 24-hydroxycholesterol	09/10	1.47E-12
Metabolism of proteins	Synthesis of glycosylphosphatidylinositol (GPI)	13/17	1.47E-12
Metabolism of proteins	N-glycan trimming in the ER and Calnexin/Calreticulin cycle	12/13	1.47E-12
Signal Transduction	Pre-NOTCH Transcription and Translation	14/19	1.47E-12
Signal Transduction	The canonical retinoid cycle in rods (twilight vision)	13/16	1.47E-12
Transmembrane transport of small molecules	Metal ion SLC transporters	21/25	1.47E-12
Transmembrane transport of small molecules	Ion transport by P-type ATPases	24/39	1.47E-12

Supplementary Figures

Figure S1: Clinical and biological characteristics in patients with and without chromothripsis

Panel (A) WBC at diagnosis in patients with (1) and without (0) chromothripsis, p = .040; panel (B) *FLT3* mutational status in patients with (1) and without (0) chromothripsis: 1 = wild-type *FLT3*, 2 = *FLT3* ITD mutation; 3 = *FLT3* TKD mutation; panel (C) Age at diagnosis in patients with (1) and without (0) chromothripsis; panel (D) ELN risk in patients with (1) and without (0) chromothripsis: 1 = LR, 2 = INT-1; 3 = INT-2; 4 = HR.

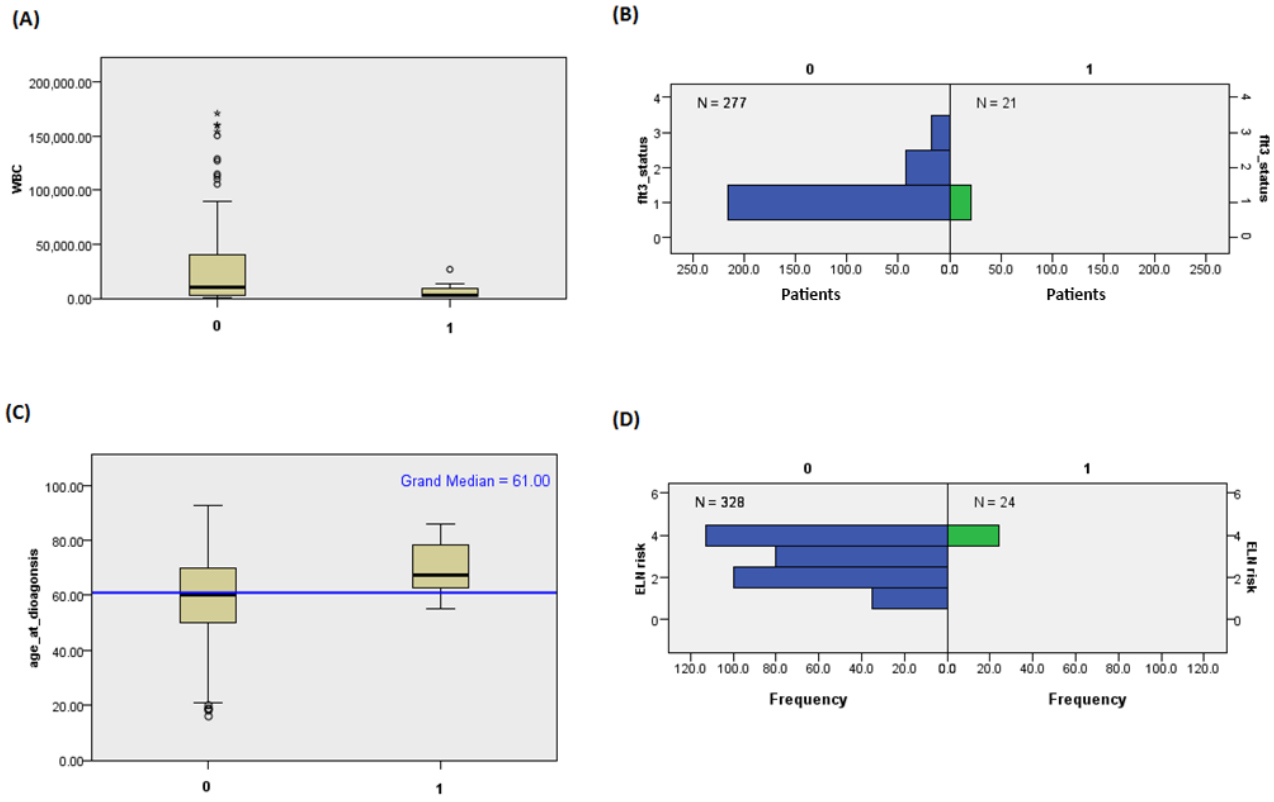

Figure S2: Representation of all chromosomes affected by chromothripsis in our cohort of adult AML patients.

Samples' IDs are reported on the top of each image representing a chromosome affected by chromothripsis: in some patients chromothripsis occurred in 2 different chromosomes. The figure is plotted with R package "Rawcopy" using R 3.3.2.

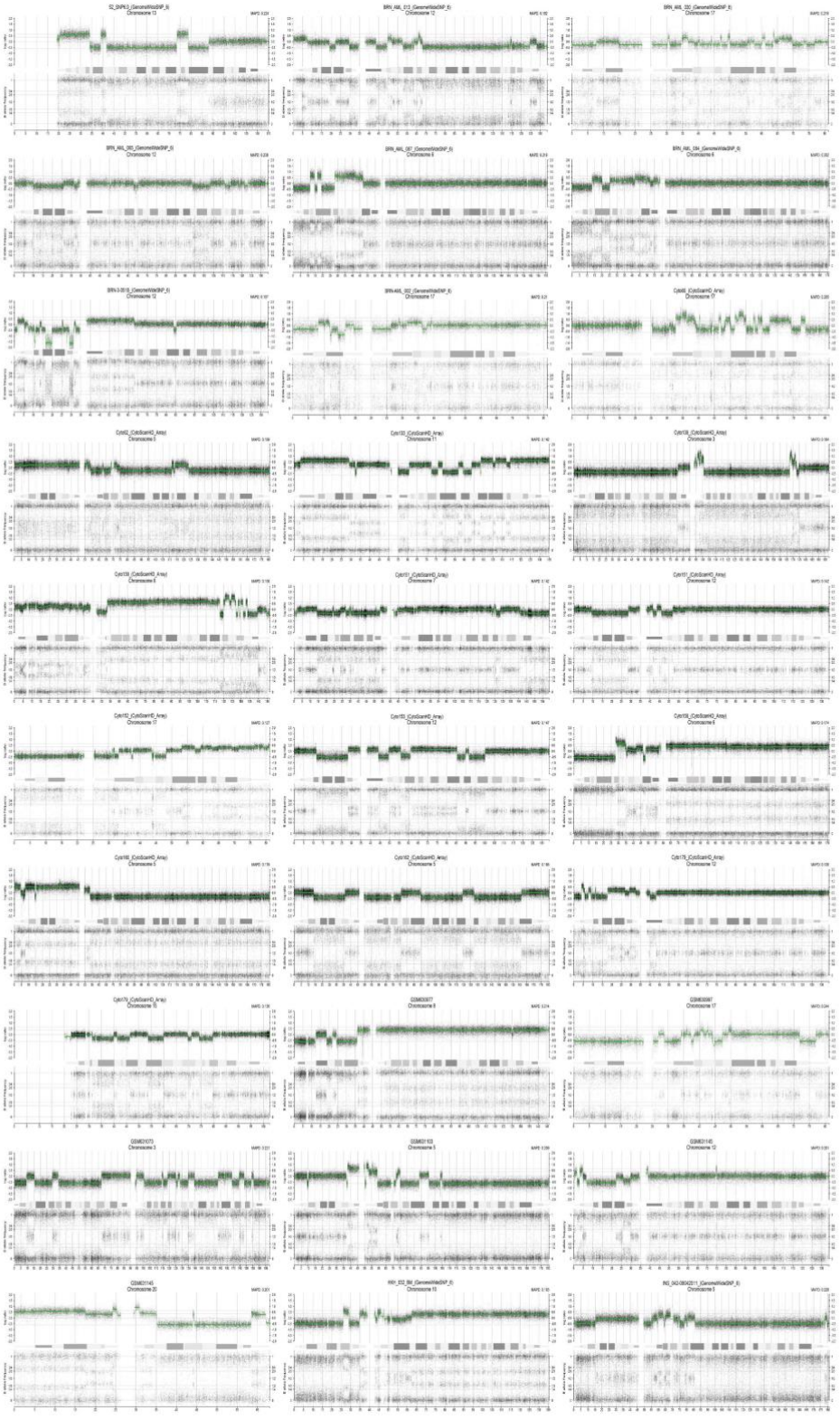

Pharmacological inhibition of WIP1 by GSK2830371 sensitizes AML cells to MDM2 inhibitor Nutlin-3a

Maria Chiara Fontana[1], Jacopo Nanni[1], Giovanni Marconi[1], Martina Pazzaglia[1], Matteo Bocconcelli[1], Antonella Padella[1], Simona Soverini[1], Ilaria Iacobucci[1,2], Cristina Papayannidis[1], Michele Cavo[1], Andrea Ghelli Luserna di Rorà [1] and Giorgia Simonetti [1] and Giovanni Martinelli[3].

[1] Institute of Hematology "L. and A. Seràgnoli", University of Bologna, Italy
[2] Present: Department of Pathology, St. Jude Children's Research Hospital, Memphis, TN, USA
[3] Istituto Scientifico Romagnolo per lo Studio e la Cura dei Tumori (IRST) IRCCS, Meldola, Italy

Manuscript in preparation

Abstract presented at AACR Annual Meeting 2018.
Cancer Research, 2018, DOI: 10.1158/1538-7445.AM2018-1872

INTRODUCTION

PPM1D (wild-type p53-inducible protein phosphatase WIP1) is a member of the PP2C family serine/threonine phosphatase involved in negative regulation of cell stress response pathways. In particular, it leads to suppression of p53 after stress. WIP1 interacts with DNA damage response pathways and plays a role in cell cycle checkpoints. *PPM1D* somatic mutations appeared to have oncogenic properties in many cancers[69]. These mutations were described in 46% of therapy-related MDS, leading to the overexpression of WIP1 and, consequently, switching off p53 activity. *PPM1D* mutations are also considered relevant for clonal hematopoiesis, and may favor leukemia onset[40]. The role of WIP1 is not well described in leukemia, but a recent study in AML showed that truncating *PPM1D* mutations confer chemoresistance, resulting in the selective expansion of *PPM1D*-mutant hematopoietic cells and that this resistance could be reverted by the allosteric inhibition of WIP1 by GSK2830371[1].

In the clinical setting, restoration of p53 function through MDM2 inhibition (Idasanutlin) is becoming a promising approach in AML, in particular for relapsed/refractory patients lacking for a real therapeutic opportunity. Promising results of the combined inhibition of MDM2 and WIP1, obtained in many preclinical studies of solid tumors, paved the way for their application in AML[66,77,78].

We here investigated whether the inhibition of WIP1 by GSK2830371 could sensitize AML cell lines and primary cells to MDM2 inhibitor (Nutlin-3a) in order to obtain a novel therapeutic strategy for AML patients, based on restoration of p53 activity.

METHODS

Leukemia cell lines

Human AML cell lines (OCI-AML3, MOLM-13, MV-4-11 and NOMO-1) were obtained from Leibniz-Institut DSMZ-Deutsche Sammlung von Mikroorganismen und Zellkulturen GmbH (Germany). Cells (MOLM-13, MV-4-11 and NOMO-1) were cultured in RPMI-1640 medium (Invitrogen, Paisley, UK), while OCI-AML3 were cultured in alpha-MEM (with ribo- and deoxyribonucleosides) (Invitrogen, Paisley, UK). Media were added with 1% l-glutamine (Sigma, St. Louis, MO), penicillin and streptomycin (Gibco, Paisley, UK) supplemented with 10%-20% fetal bovine serum (Gibco) in a humidified atmosphere of 5% CO2 at 37°C. According to the International Agency for Research on Cancer (IARC) *TP53* database (http://www-p53.iarc.fr/) and the Catalogue of Somatic Mutations in Cancer, (COSMIC, COSMIC CELL LINES PROJECT), MOLM-13, and MV-4-11 carry *FLT3-ITD* mutation and wild-type (wt) *TP53*, NOMO-1 cells have a *TP53* deletion/frameshift mutation (C242fs*5).

Primary cells

TP53-wt primary leukemic cells were obtained, upon written informed consent (HEMAOMICS protocol), from bone marrow and peripheral blood of 3 adult AML patients (2 newly-diagnosed and one relapsed) by density gradient centrifugation over Human-Lymphoprep (Nycomed UK, Birmingham). Cells were cultured with SFEM-II Medium containing 2mM L-Glutamin, 20 ng/ml rhIL3, 20 ng/ml rhIL-6, 20 ng/ml rhSCF and 20 ng/ml rhG-CSF.

Drugs

The MDM2 inhibitor (Nutlin-3a) and the WIP1 inhibitor (GSK2830371) were purchased from Sigma-Aldrich (Sigma-Aldrich Co. St. Louis, Missouri 63103 United States).

Cell viability assay

AML cell lines were firstly seeded at different concentrations without any drugs to test the number of cells alive during time, then 50.000 cells/well were seeded in 96-wells plates at 500.000 cells/mL with increasing concentrations of drugs: Nutlin-3a 0.5 μM; 1 μM; 2.5 μM; 5 μM; and GSK2830371 5 μM; 10 μM; 20μM; for 24, 48 and 72 hours (h) and incubated at 37°C. For each cell line, DMSO was used as control with the major drug-concentration per each cell line.

Cell viability was assessed in single agents and combinations by adding WST-1 reagent (Roche Applied Science, Basel, Switzerland) to the culture medium at 1:10 dilution. Cells were incubated at 37°C and the optical density was measured by microplate ELISA reader at λ450 after 3 h. All viability assays were performed in three independent replicates. The compounds' effect in term of reduction of cell viability was normalized on the samples treated with DMSO and expressed as a percentage.
The combination effect on AML primary leukemic cell's viability was assessed by counting the number of viable and non-viable cell using Trypan blue dye exclusion method. In detail, primary leukemic cells were seeded in 24-wells plates at $1x10^6$ cell/1 ml with increasing concentrations of drug (0.5, 1, 2.5, 5 μM for Nutlin-3a; 5, 10, 20 μM for GSK2830371) for 24-48 h, incubated at 37°C and the cell viability was evaluated every 24 h. GraphPad Prism 5 software (GraphPad, Avenida de la Playa La Jolla, CA USA) was used to analyze and plot the data.

Combination index analysis

To evaluate the synergism, additivity or antagonism of the co-treatment between Nutlin-3a and GSK2830371 in cell lines, the effect of both compounds in single agent and of each combinations was used to calculate the combination index (C.I.), through CompuSyn software (ComboSyn Inc.).[121]

Annexin V-Propidium Iodide staining of apoptotic cells

To evaluate combination effect in term of induction of cell apoptosis, cells were seeded in a 6-wells plates at 500.000 cells/ml and treated simultaneously with Nutlin-3a and GSK2830371 for 24 and 48h. To quantify the percentage of apoptosis, cells were harvested and stained with Annexin V-FITC/Propidium Iodide (PI) (eBioscience™ ThermoFisher Scientific) according to manufacturer's instruction. The percentage of Annexin V-PI positive cells was determined within 1×10^4 cells of the population by flow cytometry (Facs CantoII, BD Biosciences Pharmingen, San Jose, California, USA and BD Accuri C6, BD Biosciences) in three or more independent experiments. The mean percentage of Annexin V-PI positive cells and standard error measurement was calculated from at least three separate experiments. The number of apoptotic cells was evaluated considering the positivity of early and late apoptosis, excluding the percentage of necrotic cells.
GraphPad Prism 5 software (GraphPad, Avenida de la Playa La Jolla, CA USA) was used to analyze and plot the data.

RNA extraction and gene expression profiling (GEP)

RNA was isolated using TRIzol® Reagent (Invitrogen) according to manufacturer's instructions from MV-4-11 and NOMO-1 after 16h of treatment (seeded 500,000 cells/ml): this time-point was chosen to assess a moderate cells-viability and differences in genes/pathways not only related to death mechanisms, which otherwise will be increased at 24/48h post-treatment. Labeled cDNA was prepared and hybridized to Human Clariom S Assay (ThermoFisher Scientific, Affymetrix) following manufacturer's instructions. GEP data were acquired in three independent replicates.

GEP data analysis

Data were processed and analyzed using Transcriptome Analysis Console Software (version 4.0.1) with signal Space Transformation Robust Multi-Array average (sst-RMA) normalization. Two-fold and 0.05 were selected as threshold for fold change and p value and considered as significant, respectively in the supervised data analysis. Changes in gene expression were calculated over the negative control. Pathway enrichment analysis of significant genes was performed with REACTOME [102,122] (version 3.6). Calculations and graphs were obtained with Microsoft Excel 365 and SPSS (v. 25). Heatmap graph was plotted with the online tool Heatmapper.

Western Blot analysis

After 16h of treatments, 3x10 ^{6} MV-4-11 and NOMO-1 cells (2 independent experiments) were collected and lysate in KH2PO4 0.1 M (pH 7,5), Igepal 1% (NP-40), β-glicerophosphate 0,1 mM and complete protease inhibitor cocktail 1X (Roche Diagnostics). For each sample, 30 μg of proteins were fractioned on Mini-Protean TGX stain-free precast gels, blotted on nitrocellulose membranes (Bio-Rad Trans-blot turbo transfer pack) and incubated overnight with the following antibodies: anti-WIP1 (#SC20712) from Santa Cruz Biotechnology; anti-p53 (PAb 140, NB 200-103) from Novus Biological; anti-p21 WAF1/Cip1 (#2947S); anti-ATM (#2790S), anti P-ATR (S248) (#2853S), anti-ATM (D2E2) (#2873S), anti P-ATM (S1981) (#5883S), anti P-Chk1 (S317) (#12302P), anti-GADD45alpha (D17E8) (#4632S), anti P-p53 (S15) (#9284S), anti P-p53 (S15) (#9287S) from Cell Signaling; anti-53BP1 (#PA5-54565) from Thermo-Scientific; anti-Chk1 (C-term) (#1740-1); anti-MDM2 (AB-166) and anti-β-actin from Sigma-Aldrich (St. Louis, MO). Anti-rabbit and anti-mouse IgG horseradish peroxidase linked (GE Healthcare UK Limited) were used as secondary antibodies. The signal was detected using the enhanced chemiluminescence kit ECL (GE) and the compact darkroom ChemiDoc-It (UVP).

RESULTS

Idasanutlin and GSK2830371 in single agent inhibit AML cells viability

The efficacy of both compounds, in terms of reduction of cell viability, was firstly evaluated on a panel of *TP53*-wt AML cell lines (MOLM-13, MV-4-11 and OCI-AML3) and on the *TP53*-mutated NOMO-1 cell line. In order to evaluate the cytotoxicity of the two inhibitors, cells were incubated for 24, 48 and 72 h with increasing concentrations of Nutlin-3a (0.5 to 5 μM) and GSK2830371 (5 to 20 μM) (**Fig.6**). Nutlin-3a reduced the cell viability in single agent in all the treated cells in a time and dosage-dependent manner, except for NOMO-1. Independently to the cell line subtype, GSK2830371 significantly affect the cell viability only after 72h of incubation and using the highest dose (20 μM, **Fig.6**). The analysis highlighted that MOLM-13 and MV-4-11 were more sensitive than OCI-AML3, and that NOMO-1 was almost insensitive to both drugs.

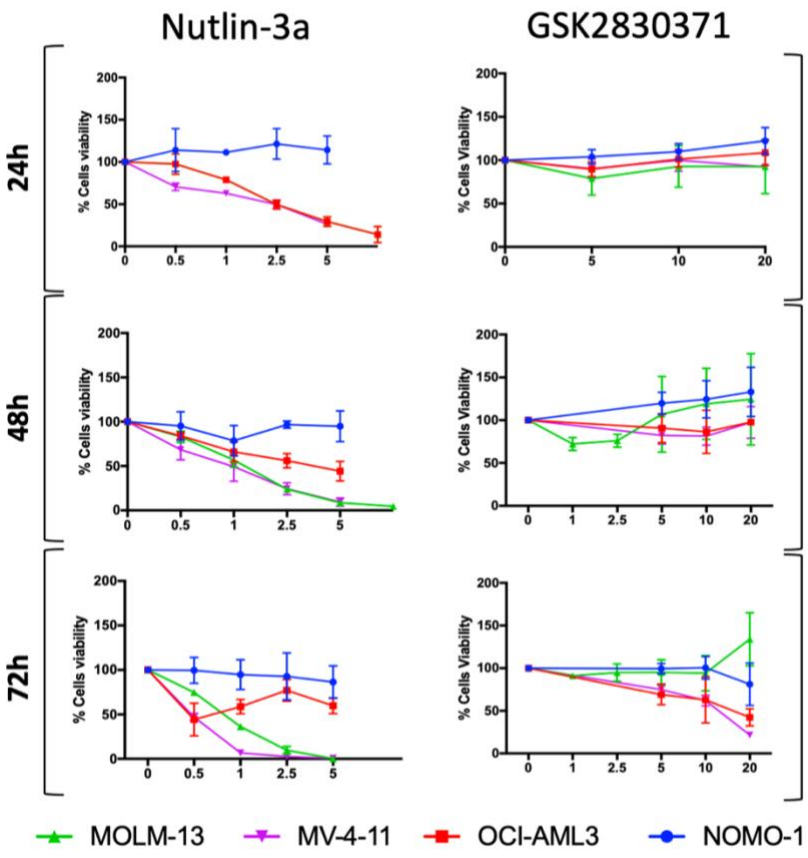

Figure 6. AML cell lines response to Nutlin-3a and GSK2830371. Plots showing the inhibition of cell viability in AML cell lines by increasing concentrations of Nutlin-3a (from 0.5 to 5 μM) and GSK2830371 (from 5 to 20 μM) as single agent at 24, 48 and 72 h.

Combined inhibition of Nutlin-3a and GSK2830371 synergistically reduces AML cells viability

The efficacy of a simultaneous inhibition of MDM2 and WIP1 was assessed by incubating the AML cell lines with Nutlin-3a (from 0.5 to 5 μM) and GSK2830371 (from 5 to 20 μM) for 24, 48 and 72 h. The co-treatment reduced the viability of the *TP53*-wt cell lines but not of the *TP53*-mutated cell line, NOMO-1. In details, OCI-AML3 confirmed to be less sensitive than MOLM-13 and MV-4-11; while NOMO-1 resulted to be insensitive to the combination (**Figure 7)**. The combination index analyses showed a synergistically effect (C.I. <1) of the combination of Nutlin-3a plus GSK2830371 in MOLM-13, MV-4-11 and OCI-AML3 (**Table 4**). On NOMO-1 the C.I. could not be calculated due to the absence of reduction of cell viability.

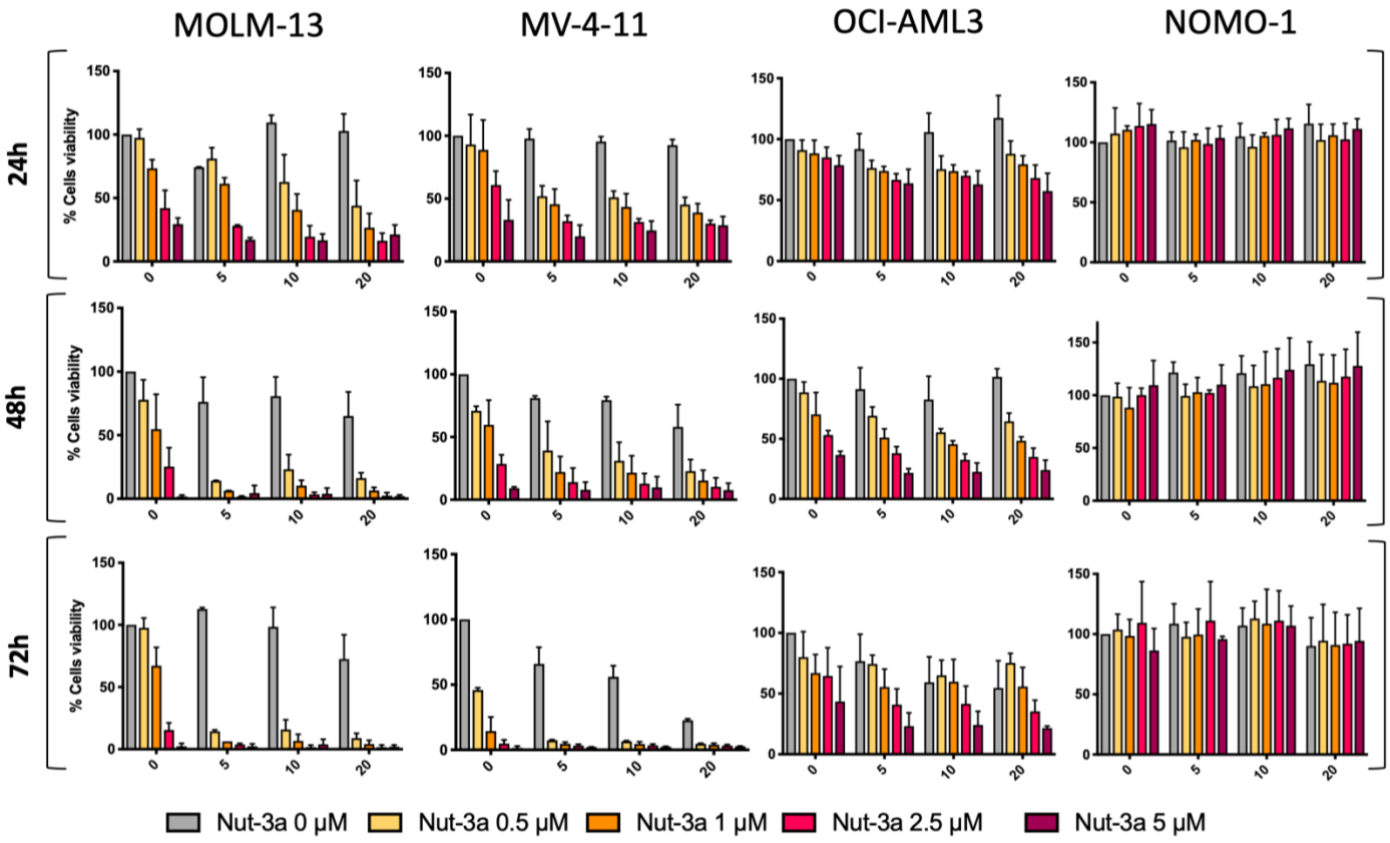

Figure 7. AML cell line response to combined Nutlin-3a and GSK2830371 treatment. Plots showing the inhibition of cell viability in AML cell lines by increasing combination of Nutlin-3a (from 0.5 to 5 μM) and GSK2830371 in X axes (from 5 to 20 μM) at 24, 48 and 72 h. (Abbreviations: Nutlin-3a as Nut-3a)

Table 4. Combination index analysis on *TP53-wt* AML cell lines

TP53-wt AML cell lines	Drug concentration [μM]		*24h*			*48h*			*72h*		
			GSK2830371								
			5	**10**	**20**	**5**	**10**	**20**	**5**	**10**	**20**
MOLM-13	**Nutlin-3a**	**0.5**	0.24	0.25	0.33	0.79	0.83	0.85	0.84	0.85	0.88
		1	0.35	0.47	0.60	0.90	0.92	0.93	0.93	0.94	0.95
		2.5	0.72	0.70	0.77	0.95	0.96	0.97	0.96	0.98	0.98
		5	0.81	0.79	0.84	0.99	0.99	0.99	0.98	0.98	0.98
MV-4-11		**0.5**	0.23	0.33	0.29	0.22	0.18	0.16	0.44	0.54	0.60
		1	0.24	0.26	0.29	0.25	0.24	0.19	0.70	0.80	0.88
		2.5	0.41	0.51	0.48	0.39	0.47	0.30	1.28	1.36	1.50
		5	0.29	0.63	0.67	0.45	0.45	0.45	2.11	2.17	2.30
OCI-AML3		**0.5**	0.06	0.08	0.33	0.30	0.25	0.66	0.87	0.77	4.88
		1	0.90	0.09	0.11	0.26	0.25	0.28	0.91	1.90	3.21
		2.5	0.11	0.15	0.09	0.38	0.35	0.31	0.86	1.25	0.92
		5	0.10	0.08	0.04	0.34	0.34	0.31	0.79	0.98	0.89

GSK2830371 sensitizes TP53-wt AML cells to Nutlin-3a-induced apoptosis

The most powerful combinations were chosen to evaluate the effect of the concomitant inhibition of MDM2 and WIP1 on the induction of cell apoptosis: 2.5 and 20 μM for OCI-AML3; 0.5 and 5 μM for MV-4-11; 0.5 and 10 μM for MOLM-13; 5 and 20 μM for NOMO-1, respectively for Nutlin-3a and GSK2830371.

The experiment showed an increased induction of cell apoptosis in all the *TP53*-wt cell lines treated simultaneously with Nutlin-3a and GSK2830371, when compared with the single treatment effect. In line with the result of the cell viability assay, no effect was seen in the *TP53*-mutated cell line in the induction of cell apoptosis (**Figure 8**).

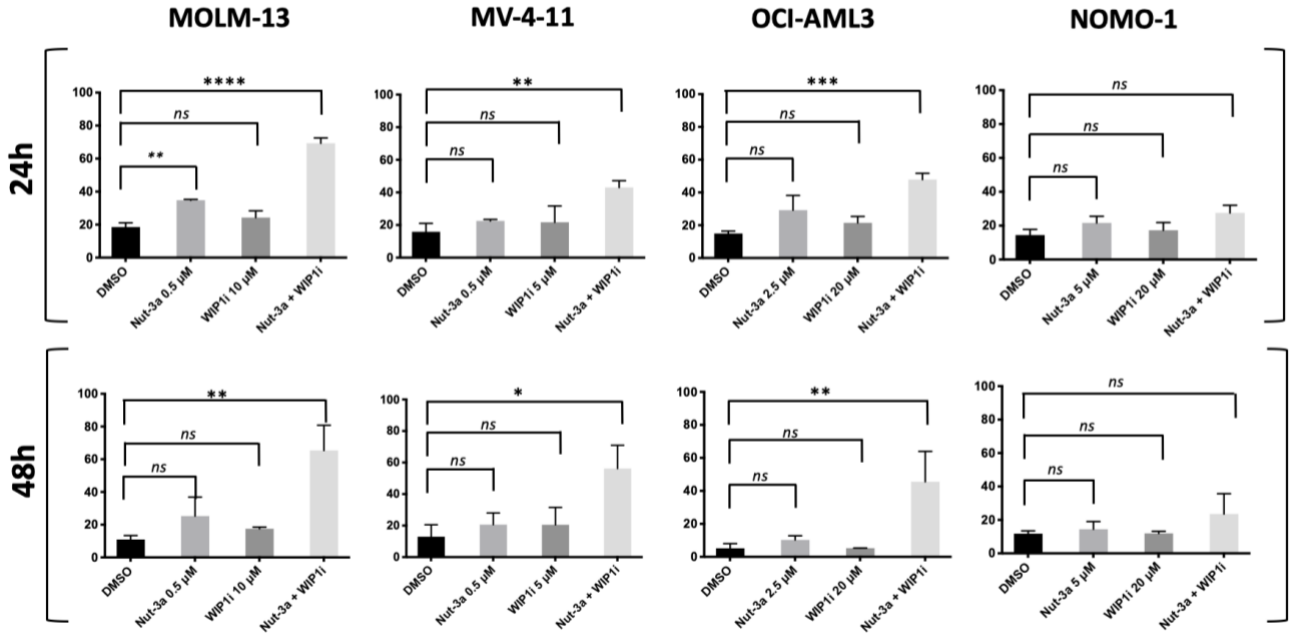

Figure 8. AML cell line apoptosis in response to combined Nutlin-3a and GSK2830371 treatment. Plots showing apoptosis analysis of AML cell lines treated for 24 and 48 h with a combined treatment of Nutlin-3a and GSK2830371. (Abbreviations: Nutlin-3a as Nut-3a; GSK2830371 as WIP1i)

The combination effect between Nutlin-3a and GSK2830371 was assessed also on wild-type *TP53* primary AML cells. The cell viability analysis confirmed the efficacy of the combination also on primary leukemic cells. In detail, primary AML cells were treated simultaneously with the two inhibitors for 24 (data not showed) and 48h (**Figure 9A**). To correlate the effect of the combination with the induction of apoptosis, primary leukemic cells were treated with Nutlin-3a with or without GSK2830371 for 24 and 48 h, and then stained with Annexin V/PI staining. The results confirmed the increased induction of cell apoptosis in the co-treated samples when compared to single agents (**Figure 9B**).

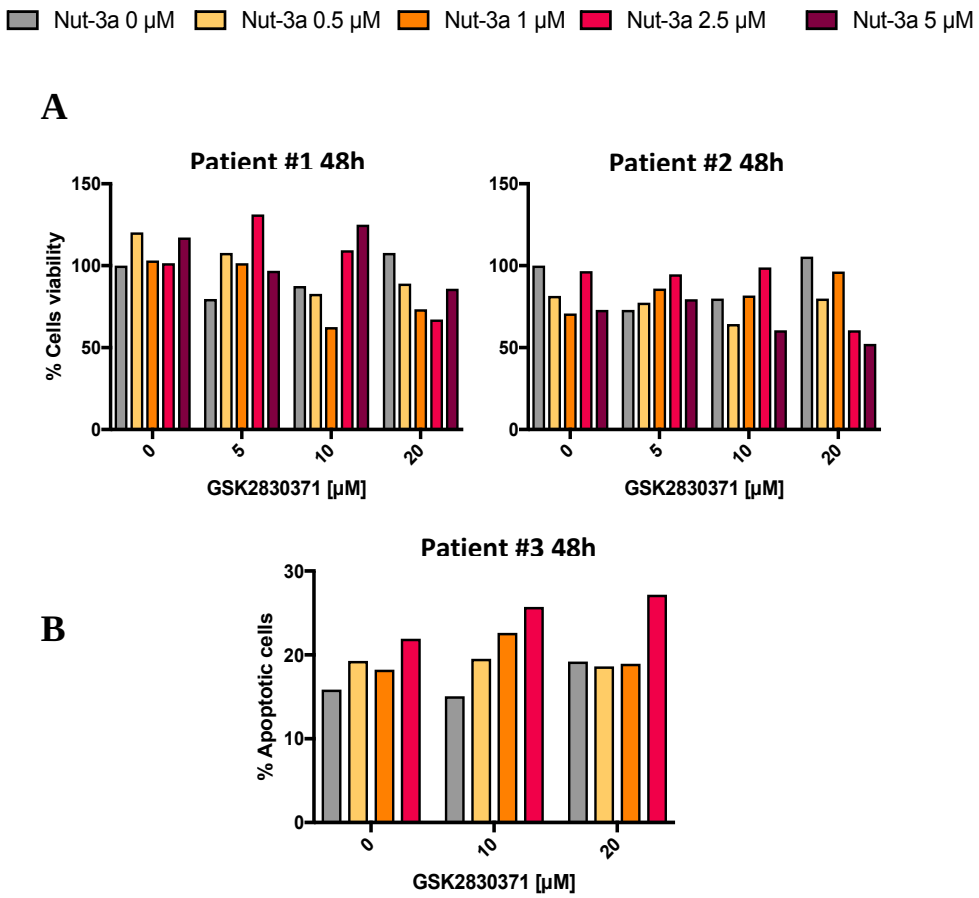

Figure 9. Primary AML cells response to combined Nutlin-3a and GSK2830371 treatment. Panel (A) showed the cells' viability percentage in 2 newly diagnosed AML (#1 and #2) treated with increasing concentration of Nutlin-3a (0,5; 1; 2.5; 5 µM) and GSK2830371 (5; 10; 20 µM) in single agents and combination. Panel (B) showed the percentage of apoptotic cells in a relapsed AML patient (#3) treated with increasing dosage of Nutlin-3a (0,5; 1; 2.5 µM) and GSK2830371 (10, 20 µM) in single agents and combination. (Abbreviations: Nutlin-3a as Nut-3a).

The simultaneous inhibition of WIP1 and MDM2 functionality affects different pathways in TP53-mutated and TP53-wt cell lines

To investigate the consequences of Nutlin-3a and GSK283037 combination treatment, we performed GEP analysis of *TP53*-wt MV-4-11 and *TP53*-mutated NOMO-1 cells after 16h of treatment with 0.5 and 5 μM Nutlin-3a or 5 and 20 μM GSK2830371 or the combination of the drugs (including vehicle control).

In MV-4-11 cells, treatment with Nutlin-3a changed the transcription of 235 genes compared with control: 174 were upregulated and 61 showed decreased expression. Top 10 upregulated and downregulated genes are listed in **Table 5**. Treatment with GSK2830371 changed the transcription of 193 genes compared with control: 130 were upregulated, 63 were downregulated (**Table 6**). Drug combination changed expression of 378 genes (251 upregulated, 127 downregulated), in particular upregulating *MDM2*, *SETBP1* and other DNA binding proteins and downregulating some SMAD family genes (**Table 7**).

In NOMO-1 cells, Nutlin-3a changed the transcription of 224 genes compared with control (108 upregulated, 116 downregulated). Overexpressed genes were involved in stress response; *MDM2* was not affected (**Table 8**). Treatment with GSK2830371 altered the expression of 248 genes compared with control (118 upregulated, 130 downregulated). CD36 and selectin L appeared among the most upregulated genes (**Table 9**). Drug combination altered the expression level of 844 genes (672 upregulated, 172 downregulated), in particular with upregulation of CD36, *IL1B* and downregulation *FANCD2* and RAS family members (**Table 10**).

Table 5: Top 10 upregulated (red) and downregulated (green) genes in MV-4-11 cells treated with Nutlin-3a vs control (DMSO)

	Gene	Function	Chr	Fold change	P value
1	*TRIM22*	tripartite motif containing 22	chr11	7.568461	0.019475
2	*COMT; MIR4761*	catechol-O-methyltransferase; microRNA 4761	chr22	6.453134	0.02448
3	*WDR27*	WD repeat domain 27	chr6	6.020987	0.036095
4	*RBM12; CPNE1*	RNA binding motif protein 12; copine I	chr20	5.578975	0.038545
5	*GANAB*	glucosidase, alpha; neutral AB	chr11	5.502167	0.03752
6	*CTSA*	cathepsin A	chr20	5.314743	0.0321
7	*XPC*	xeroderma pigmentosum, complementation group C	chr3	5.028053	0.009876
8	*GMPR2*	guanosine monophosphate reductase 2	chr14	4.958831	0.020486
9	*POLH*	polymerase (DNA directed), eta	chr6	4.958831	0.001243
10	*NOTCH2*	notch 2	chr1	4.890561	0.045905
1	*HSPB11*	heat shock protein family B (small), member 11	chr1	0.174343	0.037154
2	*SNRPG*	small nuclear ribonucleoprotein polypeptide G	chr2	0.234881	0.037929
3	*MNS1*	meiosis-specific nuclear structural 1	chr15	0.277392	0.01187

4	*POGZ*	Transcript Identified by AceView, Entrez Gene ID(s) 23126	chr1	0.297302	0.042059
5	*RPL9P7*	ribosomal protein L9 pseudogene 7	chrX	0.307786	0.049621
6	*ITGB3BP*	integrin beta 3 binding protein (beta3-endonexin)	chr1	0.327598	0.026132
7	*COA6*	cytochrome c oxidase assembly factor 6	chr1	0.332171	0.046659
8	*MBD3L2*	methyl-CpG binding domain protein 3-like 2	chr19	0.346277	0.044187
9	*BBX*	Memczak2013 ANTISENSE, coding, INTERNAL, intronic best transcript NM_020235	chr3	0.353553	0.025085
10	*TK2*	thymidine kinase 2, mitochondrial	chr16	0.358489	0.045724

Table 6: Top 10 upregulated (red) and downregulated (green) genes in MV-4-11 cells treated with GSK2830371 vs control (DMSO)

	Gene	Function	Chr	Fold change	P value
1	*TIGAR*	TP53 induced glycolysis regulatory phosphatase	chr12	10.92832	0.049602
2	*ITGAL*	integrin alpha L	chr16	10.33882	0.004708
3	*VWA8; MIR5006*	von Willebrand factor A domain containing 8; microRNA 5006	chr13	10.33882	0.042006
4	*PCCB*	propionyl-CoA carboxylase beta subunit	chr3	8.693879	0.049435
5	*ASB8*	ankyrin repeat and SOCS box containing 8	chr12	7.78124	0.018251
6	*WDR77*	WD repeat domain 77	chr1	6.727171	0.021317
7	*RBM3*	RNA binding motif (RNP1, RRM) protein 3	chrX	5.426417	0.013403
8	*SLC27A2*	solute carrier family 27 (fatty acid transporter), member 2	chr15	5.098243	0.0137
9	*ZYG11B*	zyg-11 family member B, cell cycle regulator	chr1	5.063026	0.04273
10	*EXOC3*	exocyst complex component 3	chr5	5.028053	0.011139
1	*SNRPG*	small nuclear ribonucleoprotein polypeptide G	chr2	0.193446	0.040166
2	*AXIN1*	axin 1	chr16	0.277392	0.04596
3	*EZH2*	enhancer of zeste 2 polycomb repressive complex 2 subunit	chr7	0.281265	0.032722
4	*PCDHB11*	protocadherin beta 11	chr5	0.287175	0.041213
5	*CAMTA1*	calmodulin binding transcription activator 1	chr1	0.291183	0.01026
6	*XAGE3*	X antigen family, member 3	chrX	0.291183	0.041264
7	*CENPU*	centromere protein U	chr4	0.307786	0.030172
8	*MASTL*	microtubule associated serine/threonine kinase-like	chr10	0.309927	0.024322
9	*PLD1*	phospholipase D1, phosphatidylcholine-specific	chr3	0.325335	0.000139
10	*XPO1*	exportin 1	chr2	0.329877	0.016123

Table 7: Top 10 upregulated (red) and top 10 downregulated (green) genes in MV-4-11 cells treated with combination of Nutlin-3a plus GSK2830371 vs control (DMSO)

	Gene	Function	Chr	Fold change	P value
1	*MDM2*	MDM2 proto-oncogene, E3 ubiquitin protein ligase	chr12	43.71329	4.14E-05
2	*EEF1D*	eukaryotic translation elongation factor 1 delta (guanine nucleotide exchange protein)	chr8	18.12614	0.010383
3	*EDA2R*	ectodysplasin A2 receptor	chrX	14.22148	0.038409
4	*SLC43A1*	solute carrier family 43 (amino acid system L transporter), member 1	chr11	13.36141	0.005513

5	*TIGAR*	TP53 induced glycolysis regulatory phosphatase	chr12	12.21007	0.004825
6	*TP53INP1*	tumor protein p53 inducible nuclear protein 1	chr8	11.71269	0.010431
7	*VWA8; MIR5006*	von Willebrand factor A domain containing 8; microRNA 5006	chr13	11.00433	0.024749
8	*XPC*	xeroderma pigmentosum, complementation group C	chr3	10.48315	0.000714
9	*ATAD2B*	ATPase family, AAA domain containing 2B	chr2	9.447941	0.027348
10	*ASB8*	ankyrin repeat and SOCS box containing 8	chr12	8.282119	0.026251
1	*SNRPG*	small nuclear ribonucleoprotein polypeptide G	chr2	0.166086	0.033106
2	*HSPB11*	heat shock protein family B (small), member 11	chr1	0.180491	0.033249
3	*WDR76*	WD repeat domain 76	chr15	0.184284	0.02781
4	*FAM111A*	family with sequence similarity 111, member A	chr11	0.186856	0.038083
5	*POGZ*	Transcript Identified by AceView, Entrez Gene ID(s) 23126	chr1	0.203063	0.009703
6	*CENPU*	centromere protein U	chr4	0.204476	0.007636
7	*ING2*	inhibitor of growth family member 2	chr4	0.213159	0.04719
8	*RBBP8; MIR4741*	retinoblastoma binding protein 8; microRNA 4741	chr18	0.225313	0.005158
9	*SEC16A*	SEC16 homolog A, endoplasmic reticulum export factor	chr9	0.241484	0.025761
10	*NEIL3*	nei-like DNA glycosylase 3	chr4	0.243164	0.019983

Table 8: Top 10 upregulated (red) and top 10 downregulated (green) genes in NOMO-1 cells treated with Nutlin-3a vs control (DMSO)

	Gene	Function	Chr	Fold change	P value
1	*SLC39A8*	solute carrier family 39 (zinc transporter), member 8	chr4	5.314743	0.025919
2	*ADGRE1*	adhesion G protein-coupled receptor E1	chr19	4.594793	0.013278
3	*USP12*	Transcript Identified by AceView, Entrez Gene ID(s) 219333	chr13	3.89062	0.032421
4	*TUBA3C*	tubulin, alpha 3c	chr13	3.863745	0.019106
5	*SOD2*	superoxide dismutase 2, mitochondrial	chr6	3.630077	0.001219
6	*FBXO8*	Transcript Identified by AceView, Entrez Gene ID(s) 26269	chr4	3.506423	0.013815
7	*ING3*	Transcript Identified by AceView, Entrez Gene ID(s) 54556	chr7	3.340352	0.006258
8	*PTPRE*	protein tyrosine phosphatase, receptor type, E	chr10	3.226567	0.027201
9	*C1orf21*	chromosome 1 open reading frame 21	chr1	3.20428	0.036023
10	*PLK3*	polo-like kinase 3	chr1	3.20428	0.025034
1	*SIAE*	sialic acid acetylesterase	chr11	0.160428	0.006943
2	*DCHS1*	dachsous cadherin-related 1	chr11	0.213159	0.042944
3	*HHAT*	hedgehog acyltransferase	chr1	0.213159	0.012382
4	*BRD2*	bromodomain containing 2	chr6	0.22688	0.030438
5	*RNF167*	ring finger protein 167	chr17	0.246558	0.006515
6	*INTS3*	integrator complex subunit 3	chr1	0.258816	0.021166
7	*DUS2*	dihydrouridine synthase 2	chr16	0.266093	0.025561
8	*SLC10A2*	solute carrier family 10 (sodium/bile acid cotransporter), member 2	chr13	0.266093	0.002686
9	*TMEM94 MIR6785*	transmembrane protein 94; microRNA 6785	chr17	0.266093	0.034863
10	*BCORL1*	BCL6 corepressor-like 1	chrX	0.271684	0.029553

Table 9: Top 10 upregulated (red) and top 10 downregulated (green) genes in NOMO-1 cells treated with GSK2830371vs control (DMSO)

	Gene	Function	Chr	Fold change	P value
1	*CD36*	CD36 molecule (thrombospondin receptor) Memczak2013 ANTISENSE, coding, INTERNAL, intronic best transcript	chr7	16.67945	0.006482
2	*C16orf72*	NM_014117	chr16	6.062866	0.013414
3	*SELL*	selectin L	chr1	4.316913	0.002135
4	*RRP12*	Zhang2013 ALT_ACCEPTOR, ALT_DONOR, coding, INTERNAL, intronic best transcript NM_015179	chr10	4.287094	0.009339
5	*CROCC*	Zhang2013 ALT_ACCEPTOR, ALT_DONOR, coding, INTERNAL, intronic best transcript NM_014675	chr1	4.055838	0.049339
6	*DCUN1 D4*	DCN1, defective in cullin neddylation 1, domain containing 4	chr4	3.944931	0.006649
7	*EEPD1*	endonuclease/exonuclease/phosphatase family domain containing 1	chr7	3.810552	0.02192
8	*C16orf91*	chromosome 16 open reading frame 91 Memczak2013 ANTISENSE, CDS, coding, INTERNAL, intronic, UTR3 best transcript	chr16	3.810552	0.024269
9	*LRRC58*	NM_001099678	chr3	3.810552	0.038408
10	*NVL*	nuclear VCP-like	chr1	3.655326	0.034276
1	*CSRP1*	cysteine and glycine-rich protein 1	chr1	0.157127	0.008632
2	*EPN1*	epsin 1	chr19	0.189465	0.016472
3	*CCDC92*	coiled-coil domain containing 92	chr12	0.19751	0.027348
4	*TCTN2*	tectonic family member 2	chr12	0.208772	0.036179
5	*FOXM1*	forkhead box M1	chr12	0.225313	0.047667
6	*MMACHC*	methylmalonic aciduria (cobalamin deficiency) cblC type, with homocystinuria	chr1	0.244855	0.001732
7	*EP400; SNORA49*	E1A binding protein p400; small nucleolar RNA, H/ACA box 49	chr12	0.262429	0.010999
8	*RAB37*	RAB37, member RAS oncogene family	chr17	0.275476	0.034576
9	*SLC37A4*	solute carrier family 37 (glucose-6-phosphate transporter), member 4	chr11	0.287175	0.028095
10	*AURKB*	aurora kinase B	chr17	0.289172	0.019845

Table 10: Top 10 upregulated (red) and top 10 downregulated (green) genes in NOMO-1 cells treated with combination of Nutlin-3a plus GSK2830371vs control (DMSO)

	Gene	Function	Chr	Fold change	P value
1	*FABP4*	fatty acid binding protein 4, adipocyte	chr8	111.43047	0.0001159
2	*CD36*	CD36 molecule (thrombospondin receptor)	chr7	41.932589	0.0181867
3	*TNFRSF9*	tumor necrosis factor receptor superfamily, member 9	chr1	34.059846	0.0017378
4	*LACC1*	laccase (multicopper oxidoreductase) domain containing 1	chr13	32.672388	0.0193077
5	*CXCL8*	chemokine (C-X-C motif) ligand 8	chr4	31.34145	0.0067433
6	*IL7R*	interleukin 7 receptor	chr5	17.508699	0.0072519
7	*IL1B*	interleukin 1 beta	chr2	17.387758	0.0175671
8	*CCL3*	chemokine (C-C motif) ligand 3	chr17	17.267652	1.38E-05

9	*BIRC3*	baculoviral IAP repeat containing 3	chr11	16.449821	0.0203686
10	*SLC7A11*	solute carrier family 7 (anionic amino acid transporter light chain, xc- system), member 11	chr4	13.086433	0.0401755
		Fanconi anemia complementation group D2		0.41754396	0.01724527
1	*FANCD2*		chr3		
2	*LPCAT4*	lysophosphatidylcholine acyltransferase 4	chr15	0.2348807	0.0369077
3	*PACS2*	phosphofurin acidic cluster sorting protein 2	chr14	0.2431637	0.0296354
4	*ART3*	ADP-ribosyltransferase 3	chr4	0.2431637	0.0079304
5	*CA11*	carbonic anhydrase XI	chr19	0.25	0.0038047
6	*DEFB1*	defensin, beta 1	chr8	0.2660925	0.009789
7	*HIST1H3 A*	histone cluster 1, H3a	chr6	0.2679434	0.0275002
8	*AXIN1*	axin 1	chr16	0.2851909	0.0140587
9	*RASL11 A*	RAS-like, family 11, member A	chr13	0.2952482	0.0033111
10	*KNOP1*	lysine-rich nucleolar protein 1	chr16	0.301452	0.0469175

Combined Nutlin-3a and GSK2830371 treatment alters cell cycle, TP53 and DNA damage-related pathways

In MV-4-11 cells, pathway enrichment analysis showed that Nutlin-3a as single agent induced upregulation in *TP53*-mediated transcription of death receptors and ligands (**Table 11),** while GSK2830371 interfered with biotin metabolism, WNT signal and spindle checkpoint (**Table 12**). Drug combination interacted both with G1/S and G2/M transaction interfering with *TP53* degradation and *ATR* sensing (**Table 13** and **Figure 10**). In NOMO-1 cells, pathway enrichment showed that Nutlin-3a as single agent acts by interfering with *RUNX3* and *RAS* signaling (**Table 14**) while GSK2830371 interfered with presentation of surface antigens and RNA metabolism (**Table 15**); drug combination interacted with antigen presentation (**Table 16**).

Table 11: Top 10 enriched pathways in MV-4-11 cells treated with Nutlin-3a vs control (DMSO)

	Pathway name	P value	FDR
1	Defective LFNG causes SCDO3	0.016336	0.992578
2	Progressive trimming of alpha-1,2-linked mannose residues from Man9/8/7GlcNAc2 to produce Man5GlcNAc2	0.04174	0.992578
3	Regulation by c-FLIP	0.049468	0.992578
4	Lysosomal oligosaccharide catabolism	0.057666	0.992578
5	Defective TBXAS1 causes Ghosal hematodiaphyseal dysplasia (GHDD)	0.062239	0.992578
6	CASP8 activity is inhibited	0.075322	0.992578
7	TP53 Regulates Transcription of Death Receptors and Ligands	0.085387	0.992578
8	TALDO1 deficiency: failed conversion of Fru(6)P, E4P to SH7P, GA3P	0.091893	0.992578
9	TALDO1 deficiency: failed conversion of SH7P, GA3P to Fru(6)P, E4P	0.091893	0.992578
10	Pre-NOTCH Processing in the Endoplasmic Reticulum	0.094432	0.992578

Table 12: Top 10 enriched pathways in MV-4-11 cells treated with GSK2830371 vs control (DMSO)

	Pathway name	P value	FDR
1	Defective HLCS causes multiple carboxylase deficiency	5.26E-04	0.236521959
2	Defects in biotin (Btn) metabolism	8.89E-04	0.236521959
3	Biotin transport and metabolism	0.00326349	0.444708469
4	Peroxisomal protein import	0.003946836	0.444708469
5	Defects in vitamin and cofactor metabolism	0.004195363	0.444708469
6	Mitotic Spindle Checkpoint	0.007376125	0.582774252
7	RUNX1 regulates transcription of genes involved in WNT signaling	0.008624969	0.582774252
8	RUNX3 Regulates Immune Response and Cell Migration	0.010542265	0.582774252
9	RUNX1 regulates estrogen receptor mediated transcription	0.010542265	0.582774252
10	Deletions in the AXIN genes in hepatocellular carcinoma result in elevated WNT signaling	0.015188321	0.582774252

Table 13: Top 10 enriched pathways in MV-4-11 cells treated with combination of Nutlin-3a plus GSK2830371 vs control (DMSO)

	Pathway name	P value	FDR
1	Mitotic G1-G1/S phases	0.012372166	5.09E-06
2	Activation of the pre-replicative complex	0.002574555	7.29E-06
3	G1/S Transition	0.010727312	1.46E-05
4	Unwinding of DNA	8.58E-04	9.89E-05
5	G2/M Checkpoints	0.011013373	1.37E-04
6	Activation of ATR in response to replication stress	0.002789101	1.99E-04
7	Cell Cycle Checkpoints	0.0199528	2.01E-04
8	Orc1 removal from chromatin	0.005220625	2.03E-04
9	Regulation of TP53 Degradation	0.003075163	2.88E-04
10	S Phase	0.012801259	3.39E-04

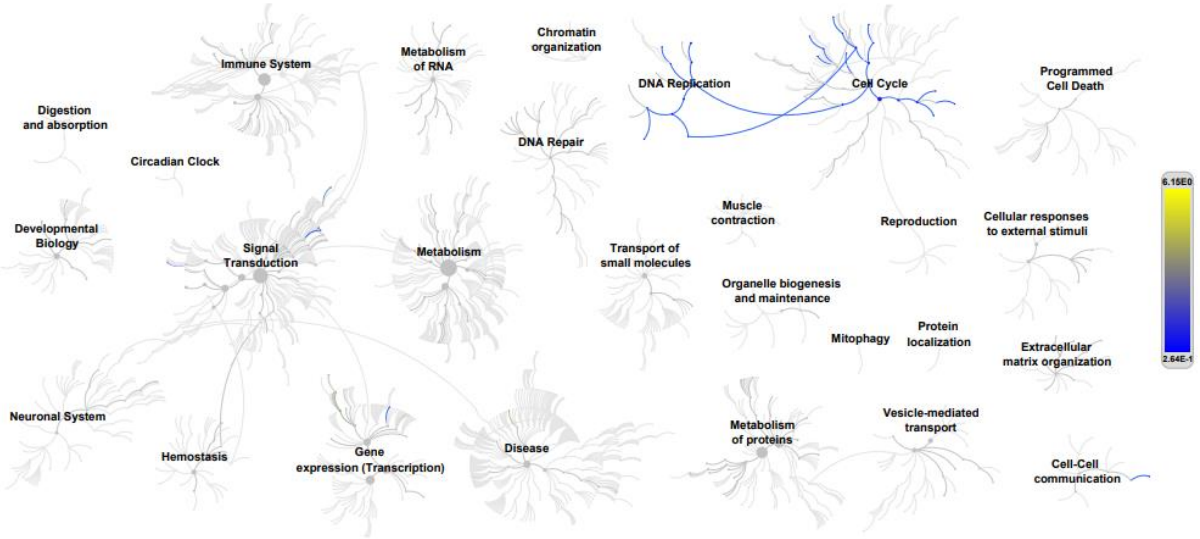

Figure 10. Genome wide view of upregulated (yellow) and downregulated (blue) pathways in MV-4-11 cells treated with combination Nutlin-3a plus GSK2830371 vs control (DMSO)

Table 14: Top 10 enriched pathways in NOMO-1 cells treated with Nutlin-3a vs control (DMSO)

	Pathway name	P value	FDR
1	CD209 (DC-SIGN) signaling	0.001960703	0.375202099
2	RUNX3 regulates RUNX1-mediated transcription	0.002429669	0.375202099
3	Signalling to ERK5	0.002429669	0.375202099
4	Diseases associated with the TLR signaling cascade	0.003110634	0.375202099
5	Diseases of Immune System	0.003110634	0.375202099
6	RUNX3 regulates p14-ARF	0.003122914	0.375202099
7	TNF receptor superfamily (TNFSF) members mediating non-canonical NF-kB pathway	0.003697208	0.375202099
8	RAS signaling downstream of NF1 loss-of-function variants	0.003752021	0.375202099
9	Gastrin-CREB signalling pathway via PKC and MAPK	0.008467964	0.419007021
10	SOS-mediated signalling	0.011600504	0.419007021

Table 15: Top 10 enriched pathways in NOMO-1 cells treated with GSK2830371 vs control (DMSO)

	Pathway name	P value	FDR
1	TICAM1-dependent activation of IRF3/IRF7	0.002896	0.549046
2	Pyrophosphate hydrolysis	0.006553	0.549046
3	MTF1 activates gene expression	0.006553	0.549046
4	Activation of IRF3/IRF7 mediated by TBK1/IKK epsilon	0.007739	0.549046
5	DDX58/IFIH1-mediated induction of interferon-alpha/beta	0.013155	0.549046
6	SUMOylation of immune response proteins	0.020643	0.549046
7	TRAF6 mediated NF-kB activation	0.020725	0.549046
8	Toll Like Receptor 3 (TLR3) Cascade	0.021133	0.549046
9	TRIF(TICAM1)-mediated TLR4 signaling	0.02199	0.549046
10	MyD88-independent TLR4 cascade	0.02199	0.549046

Table 16: Top 10 enriched pathways in NOMO-1 cells line treated with combination of Nutlin-3a plus GSK2830371 vs control (DMSO)

	Pathway name	P value	FDR
1	Interleukin-10 signaling	1.03E-06	0.001397
2	Signal regulatory protein family interactions	2.97E-04	0.193076
3	Diseases associated with the TLR signaling cascade	5.70E-04	0.193076
4	Diseases of Immune System	5.70E-04	0.193076
5	MyD88 deficiency (TLR2/4)	0.001299	0.292163
6	Interleukin-1 processing	0.001516	0.292163
7	Regulation of TLR by endogenous ligand	0.001599	0.292163
8	IRAK4 deficiency (TLR2/4)	0.001729	0.292163
9	ATF4 activates genes	0.007372	0.729285
10	Loss of MECP2 binding ability to 5hmC-DNA	0.008617	0.729285

The simultaneous inhibition of WIP1 and MDM2 affects different cluster of genes in MV-4-11 and NOMO-1

From a cluster analysis of top 150 genes expression filtered for significant FDR, we found that MV-4-11 and NOMO-1 generated a cluster per cell-line type (dendogram, **Figure 11**).

Moreover, the heatmap (**Figure 11)** representation showed the expression pattern of different gene sets cluster between TP53-mutated and TP53-wt cell lines, in particular, we found 3 different clusters. The first cluster included 66 genes upregulated in NOMO-1 treated after 16h with MDM2 and WIP1 inhibitors. This cluster included several DNA repair genes (e.g. *POLH, UBE2T, NEIL3*), G2/M transition of mitotic cell cycle (e.g. *CCNA2, CENPJ, CEP70*), the macroautophagy gene *NBR1*, the *CD36* gene and many other metabolic and signal transduction genes. In MV-4-11 sample with combined treatment these genes showed a lower expression.

Compared to NOMO-1, all samples of MV-4-11 cell line showed 2 clusters of upregulated genes, a small one with 19 genes and a bigger one with 32 genes. The first one included apoptotic (*TNFRSF9*), *TP53*-apoptotic related genes (*TIGAR*) and DNA excision and repair as *NEIL3*; the second cluster included regulators of RNA transcription (*FOSL2, MSC, EZH2*), G1/S and spindle checkpoint regulators as *FBXO5* together with several other genes involved in metabolic pathways.

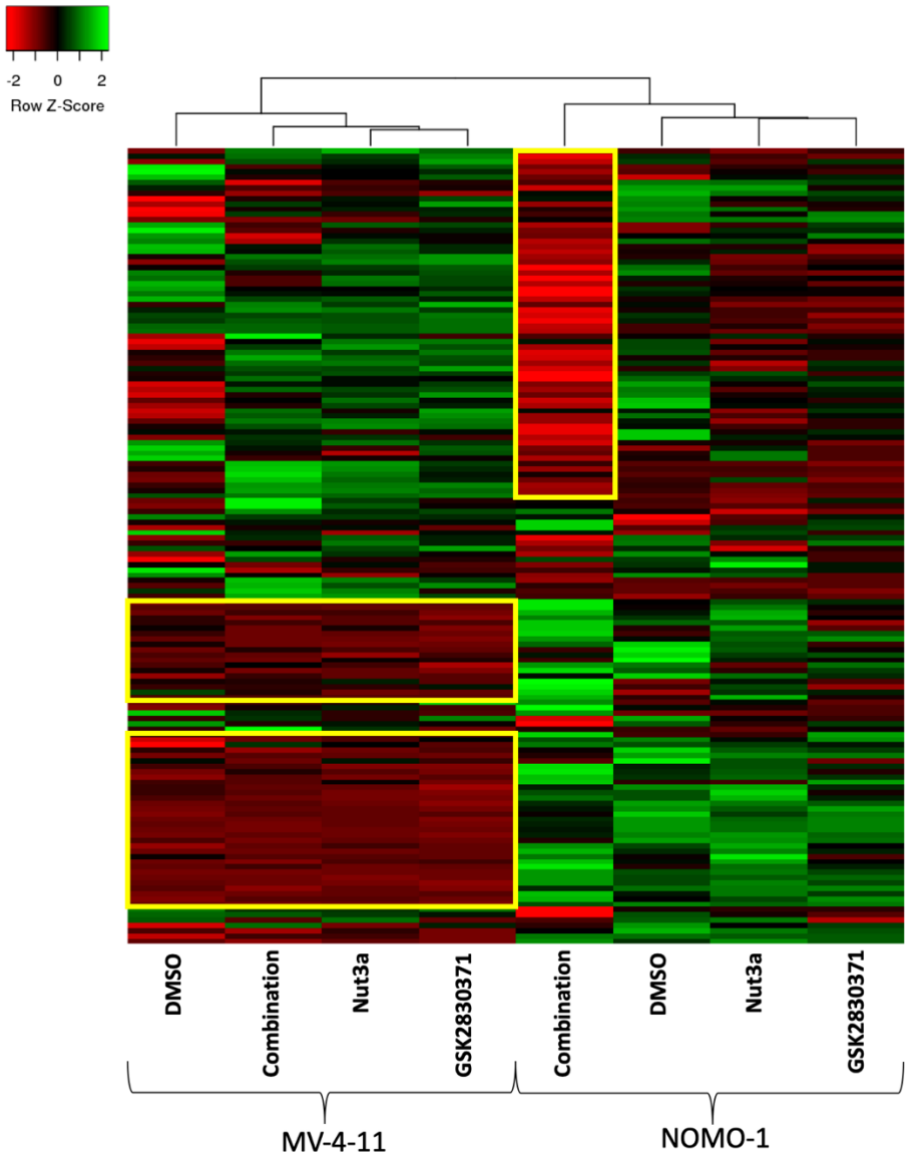

Figure 11. Heatmap representation of Top 150 filtered by best FDR score. Rows for genes, columns for samples.

Changes of TP53-related protein by Western Blots

Immunoblotting analysis **(Figure 12)** showed that in MV-4-11, p53 protein expression was synergistically increased by the co-treatment, as its downstream target p21. The expression of GADD45a showed to be higher in NOMO-1 than in MV-4-11. In NOMO-1 the basal level of p53 was not significantly affected by the treatment of the single agents, however a reduction was observed when the two drugs were used in combination.

In MV-4-11, the co-treatment also significantly reduced the basal amount of MDM2, in comparison to the single treatments and increased the level of P-p53 (Ser15); while P-p53 (Ser20) showed an increased expression in all treatment compared to control. Interestingly, 53BP1 protein showed a moderate level of expression only in NOMO-1 with single treatments.

In MV-4-11, the WIP1i and combined treatments showed an activation of P-Chk1, while the total form of Chk1 protein was reduced; in NOMO-1 the amount of Chk1 have a mild increasing in treatments versus control, while the phosphorylated form was not present.

In NOMO-1, the level of MDM2 expression was heterogeneously affected by the treatments, the amount of P-p53 (Ser15) was not detectable and the amount of and P-p53 (Ser20) was lower in WIP1i treatment.

Furthermore, NOMO-1 showed a low level of WIP1, while MV-4-11 showed a higher amount in samples that received the treatments. ATM, P-ATM (Ser1981), ATR and P-ATR (Ser428) showed a major activation and overexpression in NOMO-1, no amount was visible in MV-4-11.

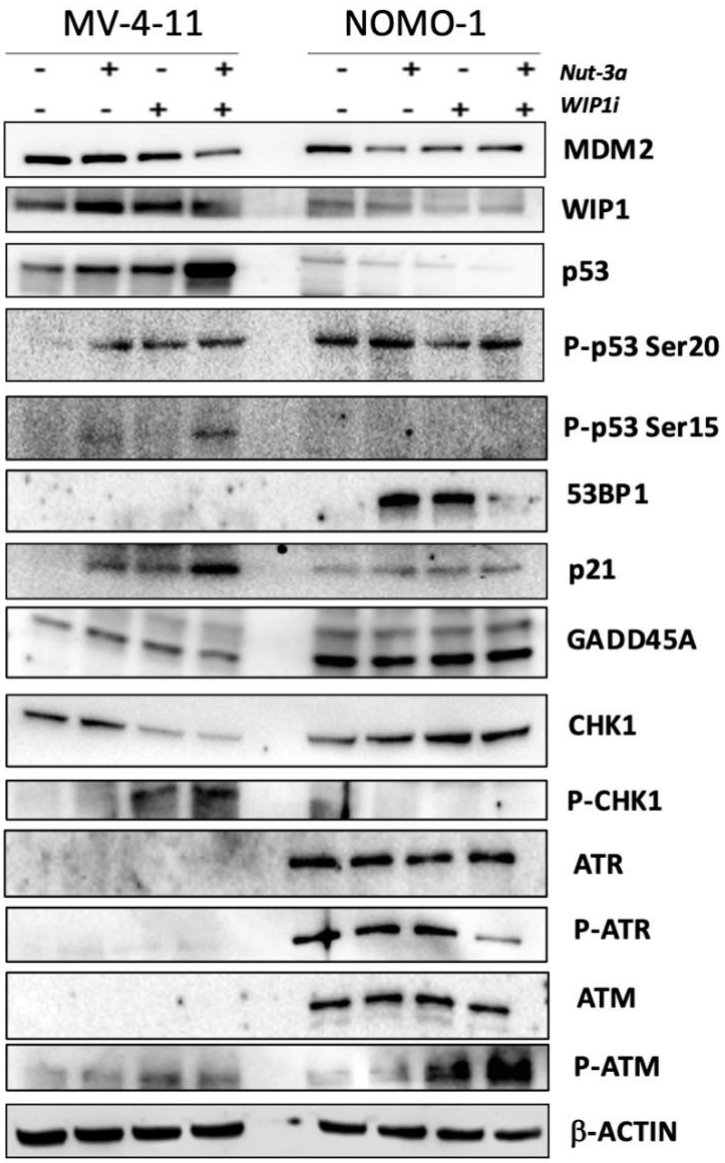

Figure 12. Western blots of MV-4-11 and NOMO-1 after 16h of exposure with Nutlin-3a and/or GSK2830371. MV-4-11: 0.5 and 5 μM; NOMO-1: 5 and 20 μM, respectively.

DISCUSSION

Our preclinical study, together with many others, confirmed the therapeutic efficacy of Nutlin-3a in *TP53*-wt AML. Several studies have proven the efficacy of Nutlin-3a in combination strategies (e.g. Idasanutlin plus Cobimetinib; Idasanutlin plus Cytarabine). Here we reported the efficacy of Nutlin-3a in combination with GSK283037, a selective WIP1 inhibitor.

PPM1D (WIP1) is an emerging oncogene involved in AML pathogenesis. It interferes with the function of p53 in response to cellular stress and DNA damage. In particular, mutations in the last exon of *PPM1D* confer chemoresistance to cytarabine, which is reversible by the inhibition of WIP1[1]. Thus, switching off WIP1 could be a promising therapy in AML to restore the activity of p53-related pathways. We show that the pharmacological inhibition of WIP1 by GSK2830371 synergistically enhances the sensitivity to MDM2 inhibitor in *TP53*-wt AML.

The gene expression changes induced by Nutlin-3a administration in our experimental setting were comparable with those reported in literature in responding and non-responding conditions[123–126]. As far as we know, this is the first report of GEP of AML cell lines receiving the WIP1 antagonist GSK2830371 in combination with an MDM2 inhibitor (Nutlin-3a).

We demonstrated by fold change analysis, pathway enrichment and gene-set cluster analyses that MV4-11 and NOMO-1 are well distinguished by cell-line type cluster and that MV-4-11 showed 2 clusters of major response to drugs with an upregulation of cell cycle control genes and TP53-dependent apoptotic mechanism compared to NOMO-1. Then, NOMO-1 co-treated with MDM2 and WIP1 inhibitor showed an overexpression of some DNA repair machinery genes, which were downregulated instead in MV-4-11. NOMO-1 cells also upregulated CD36 in response to WIP1 inhibition and to the drug combination. This is consistent with a physiological mechanism present in macrophages[127].

Immunoblotting analysis showed an increased expression of p53 and p21 in wt-*TP53* cell line after 16h of Nutlin-3a and GSK2830371 combined-treatment. WIP1 showed an increased expression in all the treated samples, while its expression was very low in all NOMO-1 samples, probably for a feedback-regulatory mechanism induced by the presence of mutated p53. Interestingly, in NOMO-1, a moderate amount of P-p53 (S20) and 53BP1 appeared, suggesting a mechanism of compensation induced by a small amount of p53. In MV-4-11, the co-treatment significantly increased the level of P-p53 (Ser15) and P-Chk1, direct target of WIP1.

We observed an upregulation of RNA level *MDM2* (Table 7) in MV-4-11 co-treated with MDM2 and WIP1 inhibitor versus control, confirming the activation of the p53 pathway. The increase of *MDM2* mRNA expression is an early marker of response to Nutlin-3a[125]. This result is in contrast to WB analyses, where the level of MDM2 protein was reduced, highlighting that post transcriptional mechanism are also involved in its regulation and that a p53-mediated apoptosis is started.
Then, the high level of ATM and ATR in NOMO-1 compared to MV-4-11, where no amount of proteins was detected, confirmed the GEP data where DNA repair genes are upregulated in TP53-mutated cells suggesting a mechanism of resiliency.

We here propose a novel synergistic drug combination between Nutlin-3a and GSK283037 that induces apoptosis in AML cell lines and primary samples. GEP and WB of *TP53*-wt MV-4-11 and *TP53*-mutated NOMO-1 cell lines showed mechanisms underlying drug sensitivity and resistance giving novel insights on potential markers of response and novel drugable targets. *In vivo* studies are needed to confirm these preclinical data.

CONCLUSIONS

In this PhD thesis, we focused on the effects of mutant *TP53* (chromothripsis-related) and on mechanisms underlying non-mutational p53 inactivation, as the activity of WIP1 and MDM2 proteins in switching off p53 functions, which might be of therapeutic in p53-based AML therapy.

Firstly, we described for the first time a peculiar mechanism of genomic instability called chromothripsis, in a big cohort of 395 newly-diagnosed adult AML patients, its impact on survival and its genomic background, using microarray. Chromothripsis is strongly associated with *TP53* mutations, even if we cannot exclude that chromothripsis may be a phenotypical manifestation, or simply an epiphenomenon, of *TP53* alteration. Larger cohorts are needed to compare patients with chromotripsis in the presence or absence of *TP53* alterations. Chromothripsis defined a group of patients with a worse OS even compared with HR patients, and significantly defined prognosis in a COX-HR optimal regression model. Chromothripsis-positive patients presented the hallmarks of chromosome instability (i.e. *TP53* alteration, 5q deletion, a higher mean of CNA, *FANCA* deletion, complex karyotype, alterations in DNA repair and cell cycle). CBA and FISH showed that chromothripsis was associated with marker, derivative and ring chromosomes.

Then, we investigated whether the inhibition of WIP1 by GSK2830371 could increase the sensitivity to MDM2 inhibitors (Nutlin-3a) in order to obtain a novel therapeutic strategy for AML patients, based on the restoration of p53 activity. We demonstrated that the pharmacological inhibition of WIP1 is able to synergistically potentiate the sensitivity to MDM2 inhibitors in AML cell lines and primary samples, by stabilizing the activity of p53, activating apoptosis and other p53-downstreams genes (e.g. *CDKN1A*) and pathways, confirmed by GEP and WB of the treated AML cells. Further *in vivo* studies are needed to confirm these preclinical data and to study GSK2830371 efficacy and toxicity, because it has never been used in the clinical practice.

The resolution of mechanisms underlying p53 dysfunction will better address the p53-targeted therapies that are currently under evaluation for AML patients, in order to overcome the mechanism of chemoresistance along with newer approaches aiming to improve the CR rates and provide a tailored treatment.

BIBLIOGRAPHY

1. Kahn, J. D. *et al.* PPM1D truncating mutations confer resistance to chemotherapy and sensitivity to PPM1D inhibition in hematopoietic cells. *Blood* blood-2018-05-850339 (2018). doi:10.1182/blood-2018-05-850339
2. Döhner, H., Weisdorf, D. J. & Bloomfield, C. D. Acute Myeloid Leukemia. *N. Engl. J. Med.* **373,** 1136–1152 (2015).
3. De Kouchkovsky, I. & Abdul-Hay, M. 'Acute myeloid leukemia: A comprehensive review and 2016 update'. *Blood Cancer J.* **6,** (2016).
4. Takahashi, S. Current findings for recurring mutations in acute myeloid leukemia. 1–11 (2011).
5. Gilliland, D. G. & Griffin, J. D. Review article The roles of FLT3 in hematopoiesis and leukemia. **100,** 1532–1543 (2018).
6. Swerdlow SH, Campo E, Harris NL, et al. WHO Classification of Tumours of Haematopoietic and Lymphoid Tissues. 4th ed. Lyon, France: IARC Press; 2008. World Health Organization Classification of Tumours; vol 2. *World Heal. Organ. Classif. Tumours; vol 2* (2008).
7. Döhner, H. *et al.* Diagnosis and management of AML in adults: 2017 ELN recommendations from an international expert panel. *Blood* **129,** (2017).
8. Vardiman, J. W. *et al.* The 2008 revision of the World Health Organization (WHO) classification of myeloid neoplasms and acute leukemia : rationale and important changes. **114,** 937–952 (2018).
9. Arber, D. A. *et al.* The 2016 revision to the World Health Organization classification of myeloid neoplasms and acute leukemia. *Blood* **127,** (2016).
10. Elli Papaemmanuil, Ph.D., Moritz Gerstung, Ph.D., Lars Bullinger, M.D., Verena I. Gaidzik, M. D., Peter Paschka, M.D., Nicola D. Roberts, B.Sc., Nicola E. Potter, Ph.D., Michael Heuser, M.D., Felicitas Thol, M.D., Niccolo Bolli, M.D., Ph.D., Gunes Gundem, Ph.D., Peter Van Loo, Ph.D., Inigo Martincorena, Ph.D., Peter Ganly, B.M., B.Ch., Ph.D., Laura Mu, B. S. & Keiran Raine, M.Sc., David R. Jones, M.Sc., Jon W. Teague, B.Sc., Adam P. Butler, B.Sc., Mel F. Greaves, Ph.D., Arnold Ganser, M.D., Konstanze Döhner, M.D., Richard F. Schlenk, M.D., Hartmut Döhner, M.D., and Peter J. Campbell, M.B., Ch.B., P. D. Genomic Classification and Prognosis in Acute Myeloid Leukemia. *N. Engl. J. Med.* (2016). doi:10.1056/NEJMoa1516192
11. Jay P. Patel, Mithat Gönen, Ph.D., Maria E. Figueroa, M.D., Hugo Fernandez, M.D., Zhuoxin Sun, P. D., Janis Racevskis, Ph.D., Pieter Van Vlierberghe, Ph.D., Igor Dolgalev, B.S., Sabrena Thomas, B.S., Olga Aminova, B.S., Kety Huberman, B.S., Janice Cheng, B.S., Agnes Viale, Ph.D., Nicholas D. Socci, Ph.D., Adriana Heguy, P. D., Athena Cherry, Ph.D., Gail Vance, M.D., Rodney R. Higgins, Ph.D., Rhett P. Ketterling, M.D., Robert E. Gallagher, M.D., Mark Litzow, M.D., Marcel R.M. van den Brink, M.D., Ph.D., Hillard M. Lazarus, M.D., Jacob M. Rowe, M. D. & Selina Luger, M.D., Adolfo Ferrando, M.D., Ph.D., Elisabeth Paietta, Ph.D., Martin S. Tallman, M.D., Ari Melnick, M.D., Omar Abdel-Wahab, M.D., and Ross L. Levine, M. D. Prognostic Relevance of Integrated Genetic Profiling in Acute Myeloid Leukemia. *N. Engl. J. Med.* **366,** 711–723 (2012).
12. Metzeler, K. H. *et al.* Spectrum and prognostic relevance of driver gene mutations in acute myeloid leukemia. *Blood* **128,** 686–699 (2016).
13. Micol, J. B. *et al.* The role of cytogenetic abnormalities in acute myeloid leukemia with NPM1 mutations and no FLT3 internal tandem duplication. *Blood* **114,** 4601–4602 (2009).
14. Gale, R. E. *et al.* The impact of FLT3 internal tandem duplication mutant level, number, size, and interaction with NPM1 mutations in a large cohort of young adult patients with acute myeloid leukemia. *Blood* **111,** 2776–2784 (2008).
15. Linch, D. C., Hills, R. K., Burnett, A. K., Khwaja, A. & Gale, R. E. Impact of FLT3ITD mutant allele level on relapse risk in intermediate-risk acute myeloid leukemia. *Blood* **124,** 273–276 (2014).

16. Pratcorona, M. *et al.* Favorable outcome of patients with acute myeloid leukemia harboring a low-allelic burden FLT3-ITD mutation and concomitant NPM1 mutation: Relevance to post-remission therapy. *Blood* **121,** 2734–2738 (2013).
17. Schlenk, R. F. *et al.* Differential impact of allelic ratio and insertion site in FLT3-ITD-positive AML with respect to allogeneic transplantation. *Blood* **124,** 3441–3449 (2014).
18. Paschka, P. & Döhner, K. Core-binding factor acute myeloid leukemia: can we improve on HiDAC consolidation? *Hematology / the Education Program of the American Society of Hematology. American Society of Hematology. Education Program* **2013,** 209–219 (2013).
19. Paschka, P. *et al.* Secondary genetic lesions in acute myeloid leukemia with inv(16) or t(16;16): A study of the German-Austrian AMLStudy Group (AMLSG). *Blood* **121,** 170–177 (2013).
20. Jourdan, E. *et al.* Prospective evaluation of gene mutations and minimal residual disease in patients with core binding factor acute myeloid leukemia. *Blood* **121,** 2213–2223 (2013).
21. Allen, C. *et al.* The importance of relative mutant level for evaluating impact on outcome of KIT, FLT3 and CBL mutations in core-binding factor acute myeloid leukemia. *Leukemia* **27,** 1891–1901 (2013).
22. Duployez, N. *et al.* Comprehensive mutational profiling of core binding factor acute myeloid leukemia. *Blood* **127,** 2451–2459 (2016).
23. Gaidzik, V. I. *et al.* RUNX1 mutations in acute myeloid leukemia: results from a comprehensive genetic and clinical analysis from the AML study group. *J. Clin. Oncol.* **29,** 1364–1372 (2011).
24. Gaidzik, V. I. *et al.* RUNX1 mutations in acute myeloid leukemia are associated with distinct clinico-pathologic and genetic features. *Leukemia* **30,** 2160–2168 (2016).
25. Schnittger, S. *et al.* ASXL1 exon 12 mutations are frequent in AML with intermediate risk karyotype and are independently associated with an adverse outcome. *Leukemia* **27,** 82–91 (2013).
26. Metzeler, K. H. *et al.* ASXL1 mutations identify a high-risk subgroup of older patients with primary cytogenetically normal AML within the ELN Favorable genetic category. *Blood* **118,** 6920–6929 (2011).
27. Pratcorona, M. *et al.* Acquired mutations in ASXL1 in acute myeloid leukemia: Prevalence and prognostic value. *Haematologica* **97,** 388–392 (2012).
28. Dimitri A. Breems, Wim L.J. Van Putten, Georgine E. De Greef, Shama L. Van Zelderen-Bhola, Klasien B.J. Gerssen-Schoorl, Clemens H.M. Mellink, Aggie Nieuwint, Martine Jotterand, Anne Hagemeijer, H. Berna Beverloo, and B. Lo & ABSTRACT, ¨wenberg. Monosomal Karyotype in Acute Myeloid Leukemia : A Better Indicator of Poor Prognosis Than a Complex Karyotype. *J. Clin. Oncol.* **26,** 4791–4797 (2010).
29. Medeiros, B. C., Othus, M., Fang, M., Roulston, D. & Appelbaum, F. R. Prognostic impact of monosomal karyotype in young adult and elderly acute myeloid leukemia: The Southwest Oncology Group (SWOG) experience. *Blood* **116,** 2224–2228 (2010).
30. Kayser, S. *et al.* Monosomal karyotype in adult acute myeloid leukemia: Prognostic impact and outcome after different treatment strategies. *Blood* **119,** 551–558 (2012).
31. Cornelissen, J. J. *et al.* Comparative analysis of the value of allogeneic hematopoietic stem-cell transplantation in acute myeloid leukemia with monosomal karyotype versus other cytogenetic risk categories. *J. Clin. Oncol.* **30,** 2140–2146 (2012).
32. Pasquini, M. C. *et al.* Hematopoietic Cell Transplantation Outcomes in Monosomal Karyotype Myeloid Malignancies. *Biol. Blood Marrow Transplant.* **22,** (2016).
33. Tsai, C. H. *et al.* Genetic alterations and their clinical implications in older patients with acute myeloid leukemia. *Leukemia* **30,** 1485–1492 (2016).
34. Rücker, F. G. *et al.* TP53 alterations in acute myeloid leukemia with complex karyotype correlate with specific copy number alterations, monosomal karyotype, and dismal outcome. *Blood* **119,** 2114–2121 (2012).
35. Cancer Genome Atlas Research Network *et al.* Genomic and epigenomic landscapes of adult

de novo acute myeloid leukemia. *N. Engl. J. Med.* **368,** 2059–74 (2013).
36. Chen, S.-J., Shen, Y. & Chen, Z. A panoramic view of acute myeloid leukemia. *Nat. Genet.* **45,** 586–587 (2013).
37. Döhner, H., Weisdorf, D. J. & Bloomfield, C. D. Acute Myeloid Leukemia. *N. Engl. J. Med.* **373,** 1136–1152 (2015).
38. Genovese, G. *et al.* Clonal Hematopoiesis and Blood-Cancer Risk Inferred from Blood DNA Sequence. *N. Engl. J. Med.* **371,** 2477–2487 (2014).
39. Jaiswal, S. *et al.* Age-Related Clonal Hematopoiesis Associated with Adverse Outcomes. *N. Engl. J. Med.* **371,** 2488–2498 (2014).
40. Xie, M. *et al.* Age-related cancer mutations associated with clonal hematopoietic expansion. *Nat. Med.* **20,** 1472–1478 (2015).
41. Vajen, B., Thomay, K. & Schlegelberger, B. Induction of chromosomal instability via telomere dysfunction and epigenetic alterations in myeloid neoplasia. *Cancers (Basel).* **5,** 857–874 (2013).
42. Luijten, M. N. H., Lee, J. X. T. & Crasta, K. C. Mutational game changer: Chromothripsis and its emerging relevance to cancer. *Mutat. Res. - Rev. Mutat. Res.* **777,** 29–51 (2018).
43. Liu, P. *et al.* Chromosome catastrophes involve replication mechanisms generating complex genomic rearrangements. *Cell* **146,** 889–903 (2011).
44. Boeva, V. *et al.* Breakpoint features of genomic rearrangements in neuroblastoma with unbalanced translocations and chromothripsis. *PLoS One* **8,** e72182 (2013).
45. Tapia-Laliena, M. A., Korzeniewski, N., Hohenfellner, M. & Duensing, S. High-risk prostate cancer: a disease of genomic instability. *Urol. Oncol.* **32,** 1101–7 (2014).
46. Furgason, J. M. *et al.* Whole genome sequence analysis links chromothripsis to EGFR, MDM2, MDM4, and CDK4 amplification in glioblastoma. *Oncoscience* **2,** 618–28 (2015).
47. Rausch, T. *et al.* Genome sequencing of pediatric medulloblastoma links catastrophic DNA rearrangements with TP53 mutations. *Cell* **148,** 59–71 (2012).
48. Kloosterman, W. P., Koster, J. & Molenaar, J. J. Prevalence and clinical implications of chromothripsis in cancer genomes. *Curr. Opin. Oncol.* **26,** 64–72 (2014).
49. Nones, K. *et al.* Genomic catastrophes frequently arise in esophageal adenocarcinoma and drive tumorigenesis. *Nat. Commun.* **5,** 5224 (2014).
50. Przybytkowski, E. *et al.* Chromosome-breakage genomic instability and chromothripsis in breast cancer. *BMC Genomics* **15,** 579 (2014).
51. Hirsch, D. *et al.* Chromothripsis and focal copy number alterations determine poor outcome in malignant melanoma. *Cancer Res.* **73,** 1454–1460 (2013).
52. Magrangeas, F., Avet-Loiseau, H., Munshi, N. C. & Minvielle, S. Chromothripsis identifies a rare and aggressive entity among newly diagnosed multiple myeloma patients. *Blood* **118,** 675–678 (2011).
53. Bochtler, T. *et al.* Marker chromosomes can arise from chromothripsis and predict adverse prognosis in acute myeloid leukemia. *Blood* **129,** 1333–1342 (2017).
54. Mackinnon, R. N. & Campbell, L. J. Chromothripsis under the microscope: a cytogenetic perspective of two cases of AML with catastrophic chromosome rearrangement. *Cancer Genet.* **206,** 238–51 (2013).
55. Forero-Castro, M. *et al.* Genome-Wide DNA Copy Number Analysis of Acute Lymphoblastic Leukemia Identifies New Genetic Markers Associated with Clinical Outcome. *PLoS One* **11,** e0148972 (2016).
56. Ratnaparkhe, M. *et al.* Genomic profiling of Acute lymphoblastic leukemia in ataxia telangiectasia patients reveals tight link between ATM mutations and chromothripsis. *Leukemia* (2017). doi:10.1038/leu.2017.55
57. Bassaganyas, L. *et al.* Sporadic and reversible chromothripsis in chronic lymphocytic leukemia revealed by longitudinal genomic analysis. *Leukemia* **27,** 2376–2379 (2013).
58. Bertelsen, B. *et al.* A germline chromothripsis event stably segregating in 11 individuals

through three generations. *Genet. Med.* (2015). doi:10.1038/gim.2015.112
59. Fontana, M. C. *et al.* Chromothripsis in acute myeloid leukemia: Biological features and impact on survival. *Leukemia* (2017). doi:10.1038/leu.2017.351
60. Kadia, T. M. *et al. TP53* mutations in newly diagnosed acute myeloid leukemia: Clinicomolecular characteristics, response to therapy, and outcomes. *Cancer* **122,** 3484–3491 (2016).
61. Cancers, H. Role of p53 in Cell Death and Human Cancers. 994–1013 (2011). doi:10.3390/cancers3010994
62. Parkin, B. *et al.* Acquired genomic copy number aberrations and survival in adult acute myelogenous leukemia. *Blood* **116,** 4958–4967 (2010).
63. Prokocimer, M., Molchadsky, A. & Rotter, V. Dysfunctional diversity of p53 proteins in adult acute myeloid leukemia: Projections on diagnostic workup and therapy. *Blood* **130,** 699–712 (2017).
64. Hopkins, J. Wip1 , a novel human protein phosphatase that is induced in response to ionizing radiation in a p53-dependent manner. **94,** 6048–6053 (1997).
65. Lu, X., Nannenga, B. & Donehower, L. A. and abrogates cell cycle checkpoints. 1162–1174 (2005). doi:10.1101/gad.1291305.tein
66. Esfandiari, A., Hawthorne, T. A., Nakjang, S. & Lunec, J. Chemical Inhibition of Wild-Type p53-Induced Phosphatase 1 (WIP1/PPM1D) by GSK2830371 Potentiates the Sensitivity to MDM2 Inhibitors in a p53-Dependent Manner. *Mol. Cancer Ther.* **15,** 379–91 (2016).
67. Cao, R., Zhang, J., Zhang, M. & Chen, X. PPM1D regulates p21 expression via dephoshporylation at serine 123. *Cell Cycle* **14,** 641–647 (2015).
68. Jaiswal, H. *et al.* ATM/Wip1 activities at chromatin control Plk1 re-activation to determine G2 checkpoint duration. *EMBO J.* **36,** 2161–2176 (2017).
69. Oghabi Bakhshaiesh, T., Majidzadeh-A, K. & Esmaeili, R. Wip1: A candidate phosphatase for cancer diagnosis and treatment. *DNA Repair (Amst).* **54,** 63–66 (2017).
70. Lindsley, R. C. *et al.* Prognostic Mutations in Myelodysplastic Syndrome after Stem-Cell Transplantation. *N. Engl. J. Med.* **376,** 536–547 (2017).
71. Zajkowicz, A. *et al.* Truncating mutations of PPM1D are found in blood DNA samples of lung cancer patients. *Br. J. Cancer* **112,** 1114–1120 (2015).
72. Hervé, D. & Gardin, C. An update of current treatments for adult acute myeloid leukemia. *Blood* **127,** 53–62 (2016).
73. The, E. T. O. Acute myeloid leukemia patients' clinical response to idasanutlin (RG7388) is associated with pre-preatment MDM2 protein expression in leukemic blasts. 185–188 (2016).
74. Lyubomir T. Vassilev1,*, Binh T. Vu2, Bradford Graves2, Daisy Carvajal1, Frank Podlaski1, Zoran Filipovic1, N. K. In Vivo Activation of the p53 Pathway by Small-Molecule Antagonists of MDM2. *Science (80-.).* 844–848 (2004).
75. Tovar, C. *et al.* Small-molecule MDM2 antagonists reveal aberrant p53 signaling in cancer : Implications for therapy. (2006).
76. Torti, D. & Trusolino, L. Oncogene addiction as a foundational rationale for targeted anti-cancer therapy : promises and perils. 623–636 (2011). doi:10.1002/emmm.201100176
77. Wu, C. *et al.* Targeting negative regulation of p53 by MDM2 and WIP1 as a therapeutic strategy in cutaneous melanoma. *Nat. Publ. Gr.* **118,** 495–508 (2017).
78. Kojima, K., Maeda, A., Yoshimura, M., Nishida, Y. & Kimura, S. The pathophysiological significance of PPM1D and therapeutic targeting of PPM1D-mediated signaling by GSK2830371 in mantle cell lymphoma. *Oncotarget* **7,** (2016).
79. Esfandiari, A. A., Hawthorne, T. A., Nakjang, S. & Lunec, J. Title : Chemical inhibition of wild-type p53 induced phosphatase 1 (WIP1 / PPM1D) by GSK2830371 potentiates the sensitivity to MDM2 inhibitors in a p53-dependent manner. **1,** (2016).
80. Pechackova, S., Burdova, K., Benada, J., Kleiblova, P. & Macurek, L. Inhibition of WIP1 phosphatase sensitizes breast cancer cells to genotoxic stress and to MDM2 antagonist nutlin-

3. **7,** (2016).
81. Byrd, J. C. *et al.* Pretreatment cytogenetic abnormalities are predictive of induction success, cumulative incidence of relapse, and overall survival in adult patients with de novo acute myeloid leukemia: results from Cancer and Leukemia Group B (CALGB 8461). *Blood* **100,** 4325–4336 (2002).
82. Schoch, C. *et al.* Acute myeloid leukemia with a complex aberrant karyotype is a distinct biological entity characterized by genomic imbalances and a specific gene expression profile. *Genes. Chromosomes Cancer* **43,** 227–238 (2005).
83. Meyerson, M. & Pellman, D. Cancer genomes evolve by pulverizing single chromosomes. *Cell* **144,** 9–10 (2011).
84. Cai, H. *et al.* Chromothripsis-like patterns are recurring but heterogeneously distributed features in a survey of 22,347 cancer genome screens. *BMC Genomics* **15,** 82 (2014).
85. Donley, N. & Thayer, M. J. DNA replication timing, genome stability and cancer: late and/or delayed DNA replication timing is associated with increased genomic instability. *Semin. Cancer Biol.* **23,** 80–9 (2013).
86. Liu, G. *et al.* Genome chaos: survival strategy during crisis. *Cell Cycle* **13,** 528–37 (2014).
87. Mardin, B. R. *et al.* A cell-based model system links chromothripsis with hyperploidy. *Mol. Syst. Biol.* **11,** 828 (2015).
88. Maciejowski, J., Li, Y., Bosco, N., Campbell, P. J. & de Lange, T. Chromothripsis and Kataegis Induced by Telomere Crisis. *Cell* **163,** 1641–1654 (2015).
89. Jacoby, M. A. *et al.* The DNA double-strand break response is abnormal in myeloblasts from patients with therapy-related acute myeloid leukemia. *Leukemia* **28,** 1242–1251 (2014).
90. Govind, S. K. *et al.* ShatterProof: operational detection and quantification of chromothripsis. *BMC Bioinformatics* **15,** 78 (2014).
91. Korbel, J. O. & Campbell, P. J. Criteria for inference of chromothripsis in cancer genomes. *Cell* **152,** 1226–1236 (2013).
92. Stephens, P. J. *et al.* Massive genomic rearrangement acquired in a single catastrophic event during cancer development. *Cell* **144,** 27–40 (2011).
93. Kovtun, I. V, Murphy, S. J., Johnson, S. H., Cheville, J. C. & Vasmatzis, G. Chromosomal catastrophe is a frequent event in clinically insignificant prostate cancer. *Oncotarget* **6,** 29087–96 (2015).
94. Klampfl, T. *et al.* Complex Patterns of Chromosome 11 Aberrations in Myeloid Malignancies Target CBL, MLL, DDB1 and LMO2. *PLoS One* **8,** e77819 (2013).
95. Milosevic, J. D. *et al.* Clinical significance of genetic aberrations in secondary acute myeloid leukemia. *Am. J. Hematol.* **87,** 1010–6 (2012).
96. World Medical Association. World Medical Association Declaration of Helsinki. *JAMA* **310,** 2191 (2013).
97. Harris, P. A. *et al.* Research electronic data capture (REDCap)—A metadata-driven methodology and workflow process for providing translational research informatics support. *J. Biomed. Inform.* **42,** 377–381 (2009).
98. Uddin, M. *et al.* A high-resolution copy-number variation resource for clinical and population genetics. *Genet. Med.* **17,** 747–752 (2015).
99. R Core Team. R: A language and environment for statistical computing. (2016).
100. Mayrhofer, M., Viklund, B. & Isaksson, A. Rawcopy: Improved copy number analysis with Affymetrix arrays. *Sci. Rep.* **6,** 36158 (2016).
101. Marc Carlson. org.Hs.eg.db: Genome wide annotation for Human. (2016).
102. Willem Ligtenberg. reactome.db: A set of annotation maps for reactome. (2016).
103. Yu, G., Wang, L.-G., Han, Y. & He, Q.-Y. clusterProfiler: an R Package for Comparing Biological Themes Among Gene Clusters. *Omi. A J. Integr. Biol.* **16,** 284–287 (2012).
104. Yu, G. *et al.* ReactomePA: an R/Bioconductor package for reactome pathway analysis and visualization. *Mol. BioSyst.* **12,** 477–479 (2016).

105. Yoav Benjamini and Yosef Hochberg. Controlling the False Discovery Rate: A Practical and Powerful Approach to Multiple Testing on JSTOR. *J. R. Stat. Soc. Ser. B* **57,** 289–300 (1995).
106. Huret, J.-L. *et al.* Atlas of Genetics and Cytogenetics in Oncology and Haematology in 2013. *Nucleic Acids Res.* **41,** D920–D924 (2013).
107. Fabregat, A. *et al.* The Reactome pathway Knowledgebase. *Nucleic Acids Res.* **44,** D481-7 (2016).
108. *ISCN 2016 : an international system for human cytogenomic nomenclature.* (KARGER, 2016).
109. Kaplan, E. L. & Meier, P. Nonparametric Estimation from Incomplete Observations. *J. Am. Stat. Assoc.* **53,** 457–481 (1958).
110. Mantel, N. Evaluation of survival data and two new rank order statistics arising in its consideration. *Cancer Chemother. reports* **50,** 163–70 (1966).
111. D. R. Cox. Regression Models and Life-Tables. *J. R. Stat. Soc.* **34,** 187–220 (1972).
112. Estey, E. H. Acute myeloid leukemia: 2012 update on diagnosis, risk stratification, and management. *Am. J. Hematol.* **87,** 89–99 (2012).
113. Röllig, C. *et al.* Long-term prognosis of acute myeloid leukemia according to the new genetic risk classification of the European LeukemiaNet recommendations: evaluation of the proposed reporting system. *J. Clin. Oncol. Off. J. Am. Soc. Clin. Oncol.* **29,** 2758–2765 (2011).
114. Krzywinski, M. *et al.* Circos: an information aesthetic for comparative genomics. *Genome Res.* **19,** 1639–45 (2009).
115. Stengel, A. *et al.* The impact of TP53 mutations and TP53 deletions on survival varies between AML, ALL, MDS and CLL: an analysis of 3307 cases. *Leukemia* **31,** 705–711 (2017).
116. Zhang, C.-Z. *et al.* Chromothripsis from DNA damage in micronuclei. *Nature* **522,** 179–84 (2015).
117. Leibowitz, M. L., Zhang, C.-Z. & Pellman, D. Chromothripsis: A New Mechanism for Rapid Karyotype Evolution. *Annu. Rev. Genet.* **49,** 183–211 (2015).
118. Poot, M. & Haaf, T. Mechanisms of Origin, Phenotypic Effects and Diagnostic Implications of Complex Chromosome Rearrangements. *Mol. Syndromol.* **6,** 110–134 (2015).
119. Tischkowitz, M. D. *et al.* Deletion and reduced expression of the Fanconi anemia FANCA gene in sporadic acute myeloid leukemia. *Leukemia* **18,** 420–425 (2004).
120. Ghelli Luserna di Rora', A., Iacobucci, I. & Martinelli, G. The cell cycle checkpoint inhibitors in the treatment of leukemias. *J. Hematol. Oncol.* **10,** 77 (2017).
121. Chou, T. C. Drug combination studies and their synergy quantification using the chou-talalay method. *Cancer Res.* **70,** 440–446 (2010).
122. Fabregat, A. *et al.* The Reactome Pathway Knowledgebase. *Nucleic Acids Res.* **46,** D649–D655 (2018).
123. Wu, C.-E. *et al.* Targeting negative regulation of p53 by MDM2 and WIP1 as a therapeutic strategy in cutaneous melanoma. *Br. J. Cancer* **118,** 495–508 (2018).
124. Rasmussen, R. *et al.* P08.18 Replication stress as a driver of genomic instability in malignant gliomas. *Neuro. Oncol.* **19,** iii58-iii58 (2017).
125. Reis, B. *et al.* Acute myeloid leukemia patient clinical response to idasanutlin (RG7388) is associated with pre-treatment MDM2 protein expression in leukemic blasts. *Haematologica* (2016). doi:10.3324/haematol.2015.139717
126. Richmond, J. *et al.* Effective targeting of the P53-MDM2 axis in preclinical models of infant MLL-rearranged acute lymphoblastic leukemia. *Clin. Cancer Res. An Off. J. Am. Assoc. Cancer Res.* **21,** 1395–1405 (2015).
127. Tang, Y. *et al.* Wip1-dependent modulation of macrophage migration and phagocytosis. *Redox Biol.* **13,** 665–673 (2017).